

Supplementary Material

Synthesis and Anti-Angiogenic Activity of Novel c(RGDyK) Peptide-Based JH-VII-139-1 Conjugates

George Leonidis ¹, Anastasia Koukiali ¹, Ioanna Sigala ¹, Katerina Tsimarou ², Dimitris Beis ², Thomas Giannakouros ¹, Eleni Nikolakaki ¹ and Vasiliki Sarli ^{1,*}

- ¹ Department of Chemistry, Aristotle University of Thessaloniki, University Campus, 54124 Thessaloniki, Greece
² Zebrafish Disease Model Laboratory, Biomedical Research Foundation Academy of Athens, 11527 Athens, Greece
* Correspondence: sarli@chem.auth.gr

Supporting Info

LC/ESI-MS, HPLC parameters and method development	S3
¹ H-NMR and ¹³ C-NMR spectra for 2	S5
LC/ESI-MS analysis of 2	S6
¹ H-NMR and ¹³ C-NMR spectra for 3	S7
¹ H-NMR and ¹³ C-NMR spectra for 5	S8
¹ H-NMR and ¹³ C-NMR spectra for 6a	S9
LC/ESI-MS analysis of 6a	S10
¹ H-NMR and ¹³ C-NMR spectra for 6b	S11
¹ H-NMR and ¹³ C-NMR spectra for 7	S12
LC/ESI-MS analysis of 7	S13
¹ H-NMR and ¹³ C-NMR spectra for 8	S14
LC/ESI-MS analysis of 8	S15
¹ H-NMR and ¹³ C-NMR spectra for 9	S16
LC/ESI-MS analysis of 9	S17
¹ H-NMR and ¹³ C-NMR spectra for 10	S18
LC/ESI-MS analysis of 10	S19
¹ H-NMR spectra for 12 and 13	S20
¹ H-NMR and ¹³ C-NMR spectra for JH-VII-139-1	S21
ESI-HRMS analysis of JH-VII-139-1	S22
¹ H-NMR spectrum for 16	S23
¹ H-NMR and ¹³ C-NMR spectra for 17	S24

LC/ESI-MS analysis of 17	S25
¹H-NMR and ¹³C-NMR spectra for geo75	S26
LC/ESI-MS analysis of geo75	S27
¹H-NMR and ¹³C-NMR spectra for 20	S28
LC/ESI-MS analysis for 20	S29
¹H-NMR and ¹³C-NMR spectra for geo77	S30
LC/ESI-MS analysis of geo77	S31
¹H-NMR and ¹³C-NMR spectra for 22	S32
¹H-NMR and ¹³C-NMR spectra for 23	S33
ESI-MS analysis of 23	S34
¹H-NMR and ¹³C-NMR spectra for geo85	S35
LC/ESI-MS analysis of geo85	S36
¹H-NMR and ¹³C-NMR spectra for 24	S37
LC/ESI-MS analysis of 24	S38
¹H-NMR and ¹³C-NMR spectra for geo105	S39
LC/ESI-MS analysis of geo105	S40
¹H-NMR and ¹³C-NMR spectra for geo107	S41
LC/ESI-MS analysis of geo107	S42
¹H-NMR spectra for 28 and 29	S43
LC/ESI-MS analysis of 29	S44
¹H-NMR spectra for geo106	S45
LC/ESI-MS analysis of 106	S46
Chemostability Studies	S47
In vitro kinase inhibition assay	S48

LC/ESI-MS, HPLC parameters and method development

LC-MS/HPLC: LC-20AD Shimadzu connected to Shimadzu LCMS-2010EV

HPLC column: Supelco discovery C18, 5µm 250 x 4.6mm

Flow rate: 0.4 mL/min

Column temperature: 26°C

UV detector: 254, 280 nm

MS detector: 1.65kV

➤ Method 1

gradient elution 90% H₂O – 10% ACN (+0.1% formic acid) to 5% H₂O - 95% ACN (+0.1% formic acid)

Table S1. Conditions for Method 1.

time (min)	H ₂ O (% v/v conc.)	ACN (% v/v conc.)
3	90	10
22	15	85
25	10	90
29	10	90
31	5	95
37	5	95

➤ Method 2

gradient elution 90% H₂O – 10% ACN (+0.1% formic acid) to 10% H₂O - 90% ACN (+0.1% formic acid)

Table S2. Conditions for Method 2.

time (min)	H ₂ O (% v/v conc.)	ACN (% v/v conc.)
3	90	10
22	15	85
25	10	90
26	10	90

➤ Method 3

gradient elution 90% H₂O – 10% ACN (+0.1% formic acid) to 10% H₂O - 90% ACN (+0.1% formic acid)

Table S3. Conditions for Method 3.

time (min)	H ₂ O (% v/v conc.)	ACN (% v/v conc.)
3	90	10
22	15	85
25	10	90

29	10	90
----	----	----

➤ Method 4

gradient elution 90% H₂O – 10% ACN (+0.1% formic acid) to 5% H₂O - 95% ACN (+0.1% formic acid)

Table S4. Conditions for Method 4.

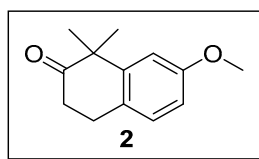
time (min)	H ₂ O (% v/v conc.)	ACN (% v/v conc.)
3	90	10
22	15	85
25	10	90
29	10	90
31	5	95
33	5	95

➤ Method 5

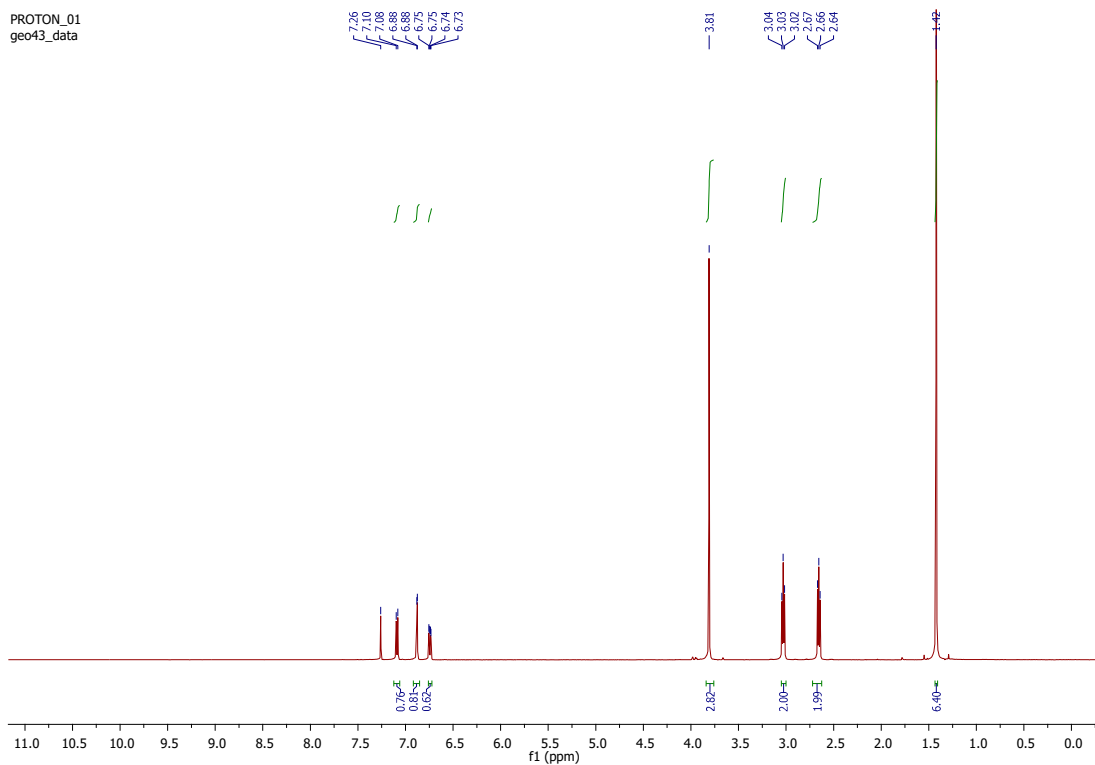
gradient elution 90% H₂O – 10% ACN (+0.1% formic acid) to 10% H₂O - 90% ACN (+0.1% formic acid)

Table S5. Conditions for Method 5.

time (min)	H ₂ O (% v/v conc.)	ACN (% v/v conc.)
3	90	10
22	15	85
25	10	90



PROTON_01
geo43_data



CARBON_01
geo43_data

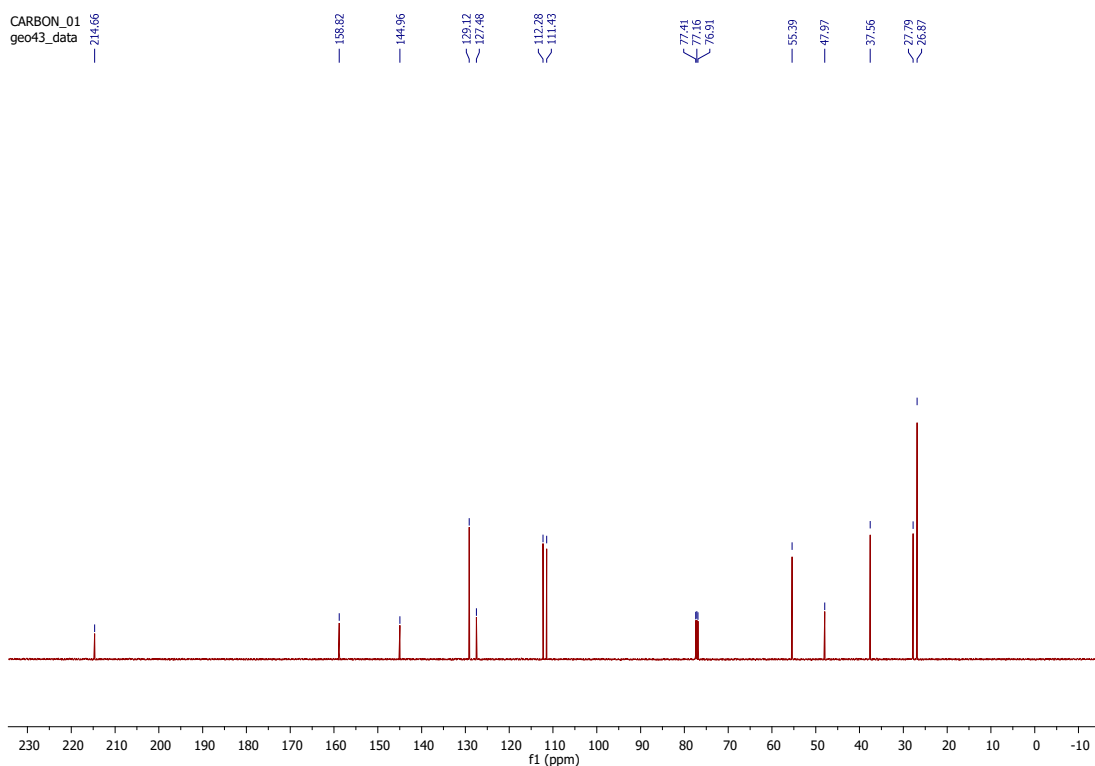
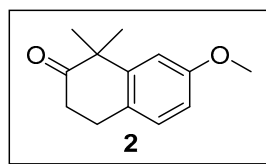


Figure S1. ¹H-NMR and ¹³C-NMR spectra for compound 2



MeOH isocratic elution

Retention time: 8.6 m

area: 1536963 (absorbance units x minutes)

total area: 1622159 (absorbance units x minutes)

area %: $(1536963/1622159) * 100 = 94.7 \%$

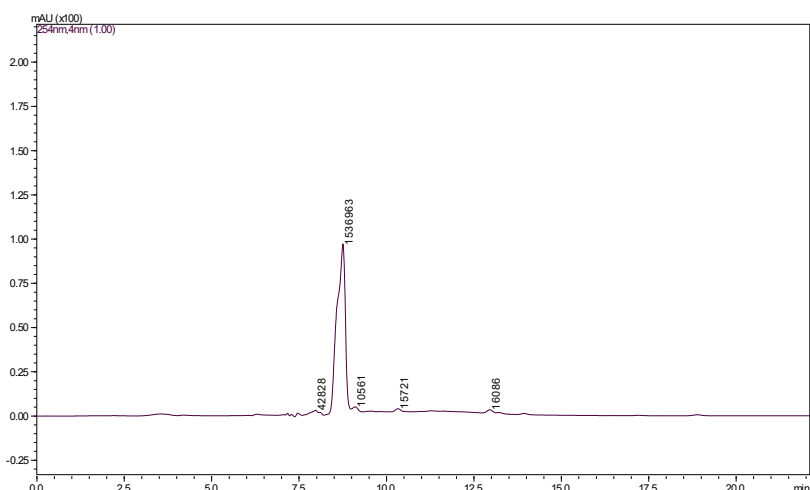


Figure S2. ESI-LCMS of compound **2** after column chromatography purification.

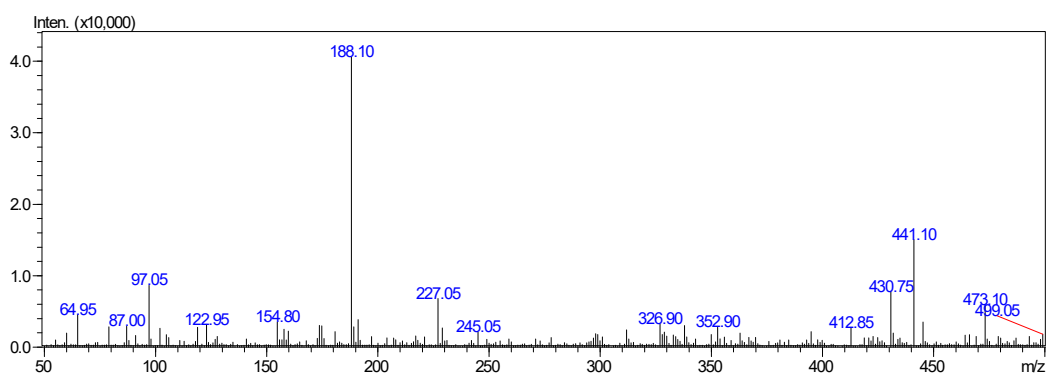


Figure S3. ESI-MS for **2**, positive mode: m/z calcd mass for $C_{13}H_{16}O_2Na [M+Na]^+$ = 227.10, was found 227.05

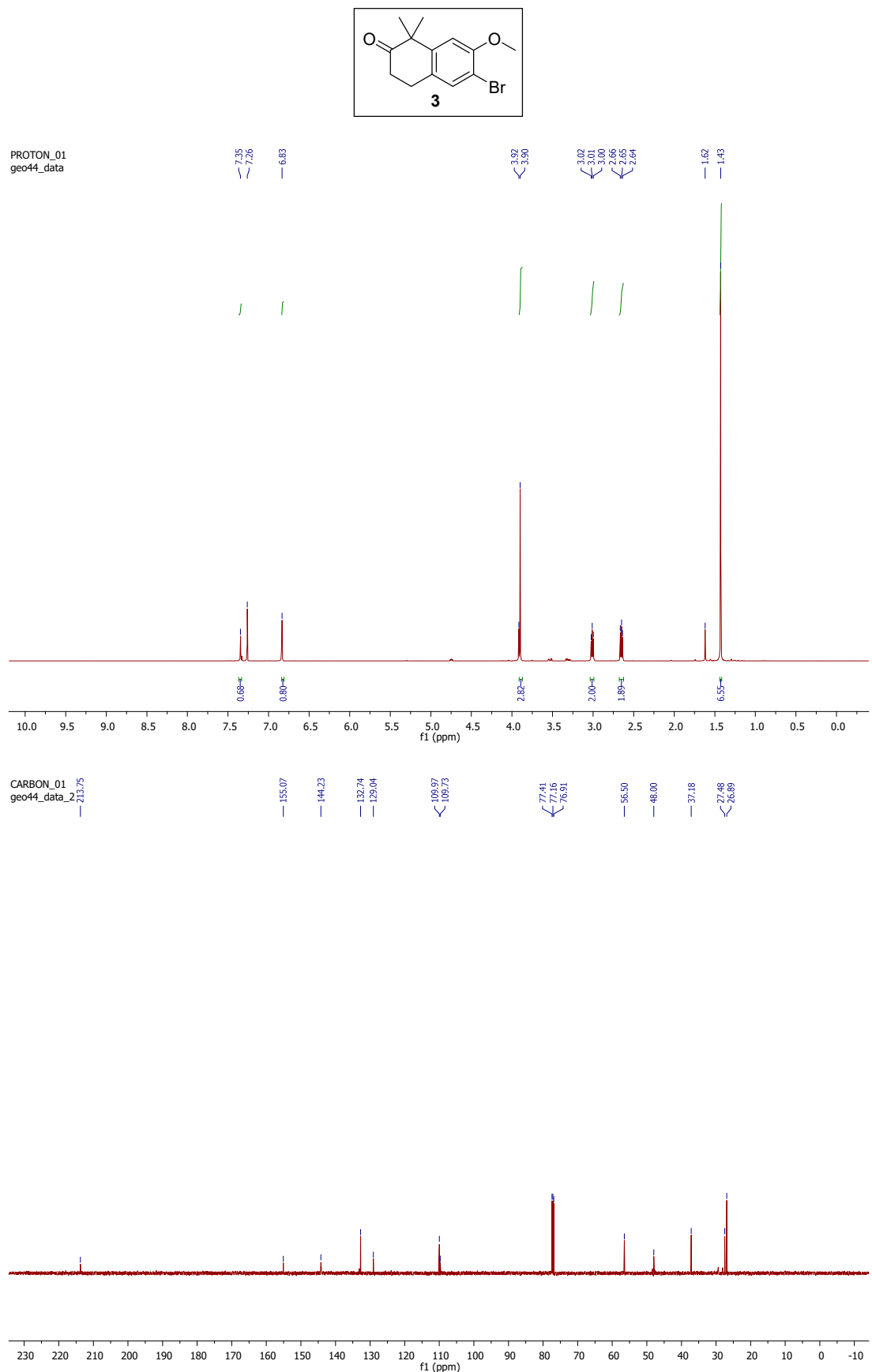


Figure S4. ^1H -NMR and ^{13}C -NMR spectra for compound **3**

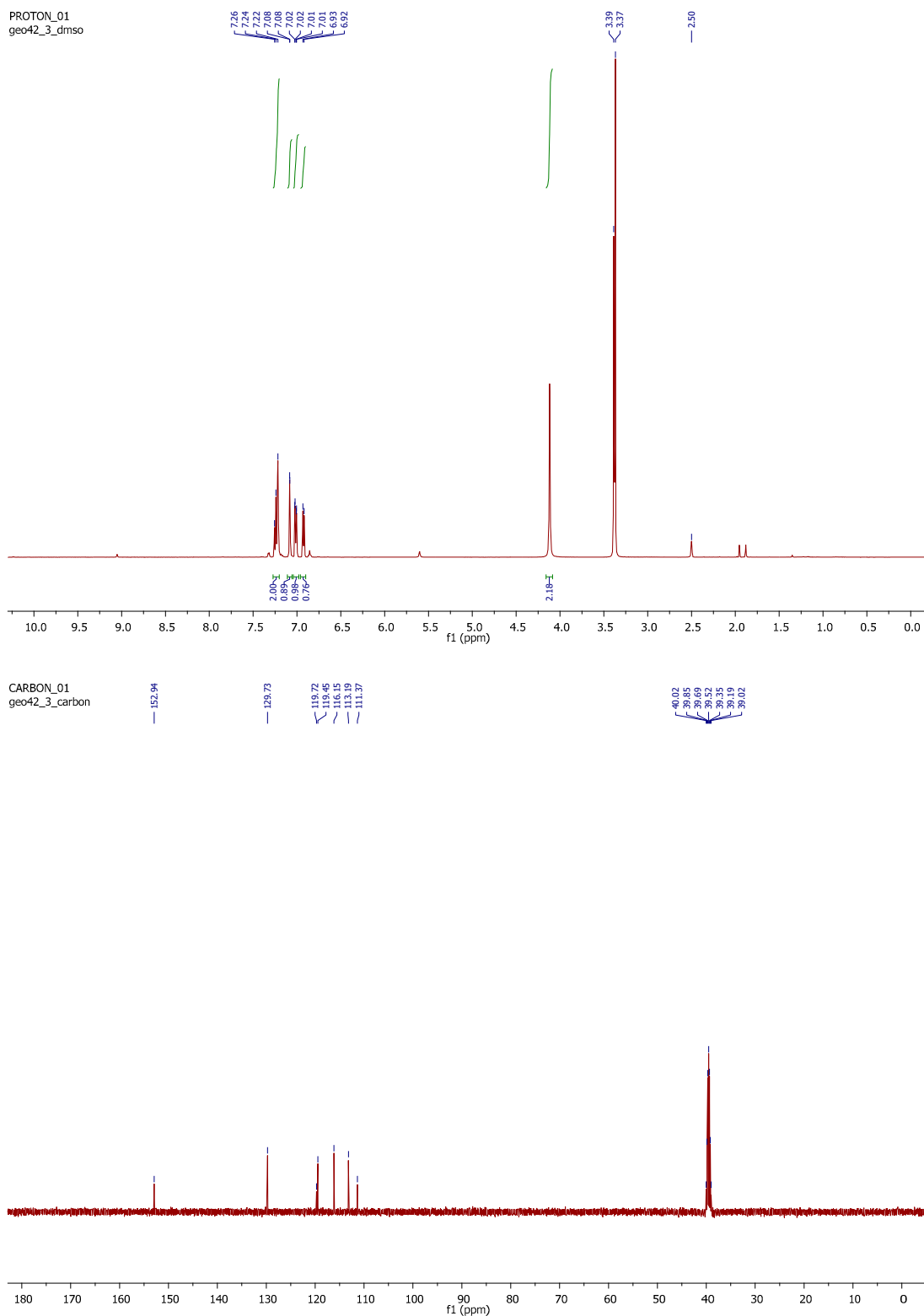
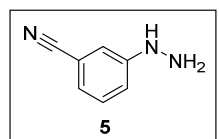


Figure S5. ^1H -NMR and ^{13}C -NMR spectra for compound **5**

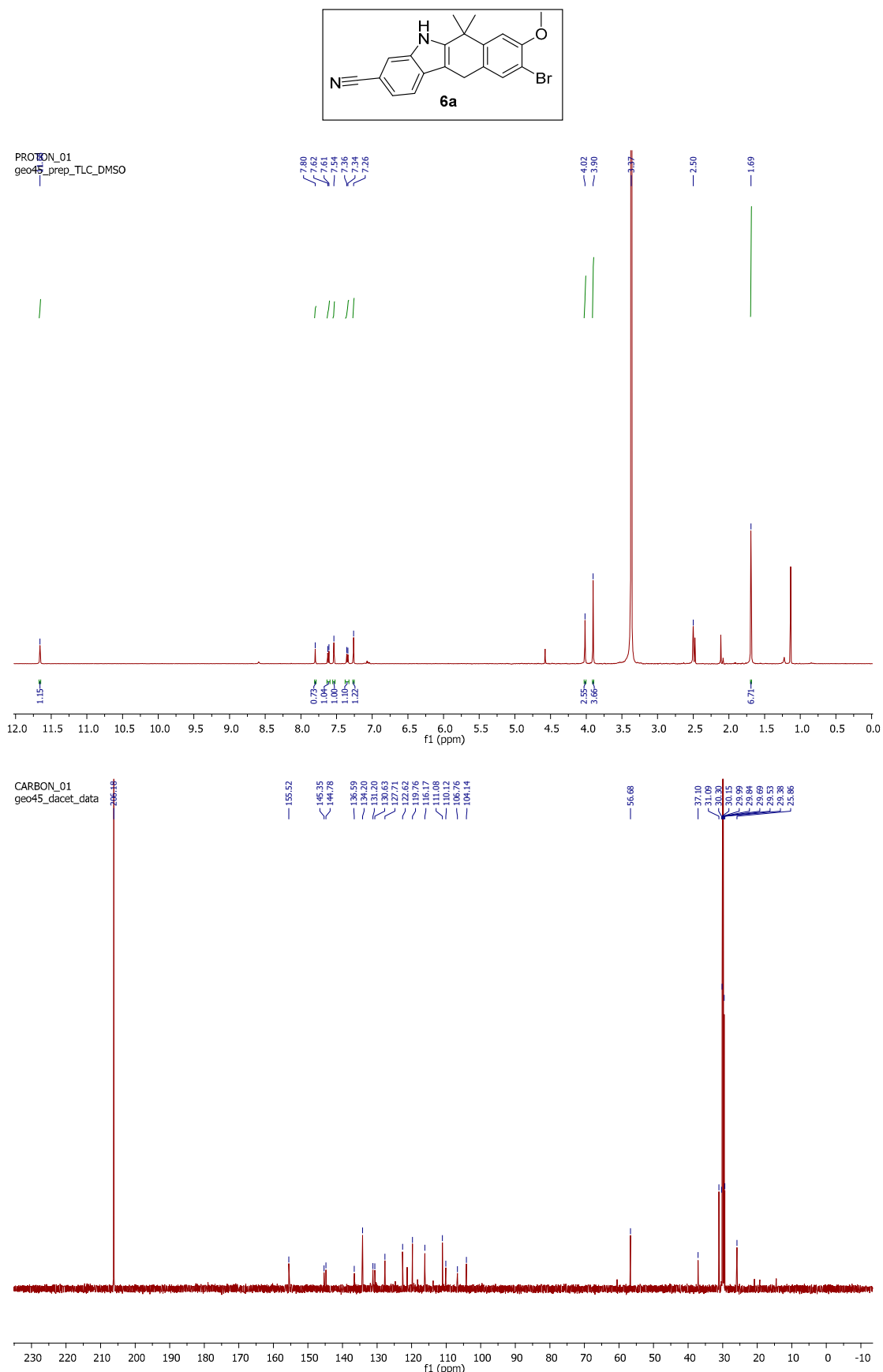
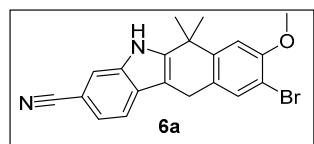


Figure S6. ^1H -NMR and ^{13}C -NMR spectra for compound **6a**



Method 1

Retention time: 32.8 m

area: 41951699 (absorbance units x minutes)

total area: 45555041 (absorbance units x minutes)

area %: $(41951699/45555041) * 100 = 92.1 \%$

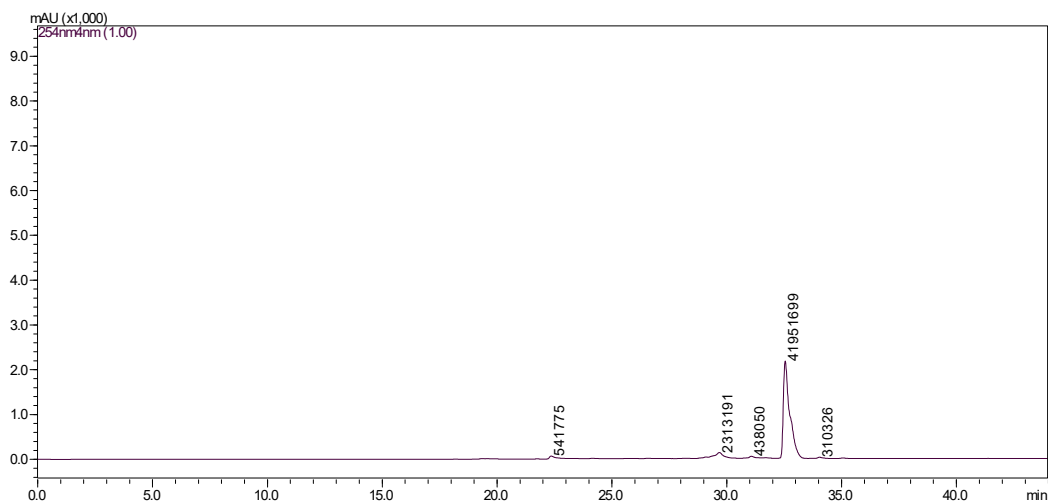


Figure S7. ESI-LCMS of compound **6a** after column chromatography purification

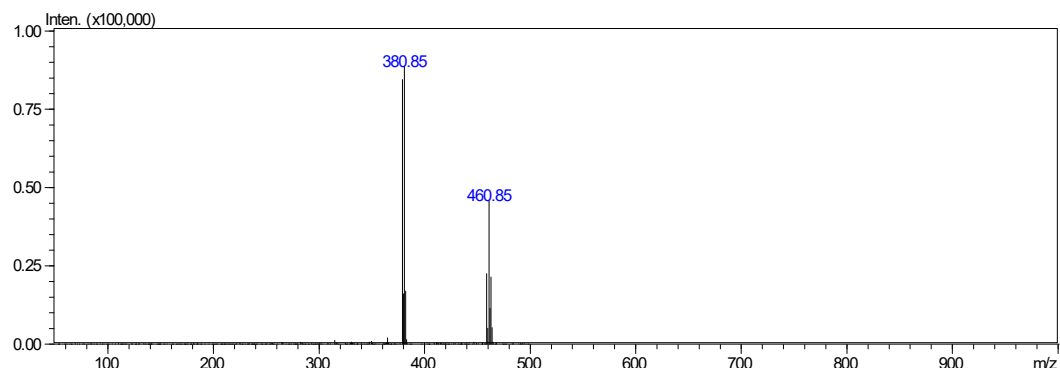


Figure S8. ESI-MS for **6a**, negative mode: m/z calcd mass for $C_{20}H_{16}BrN_2O [M-H]^-$ = 379.04, was found 380.85

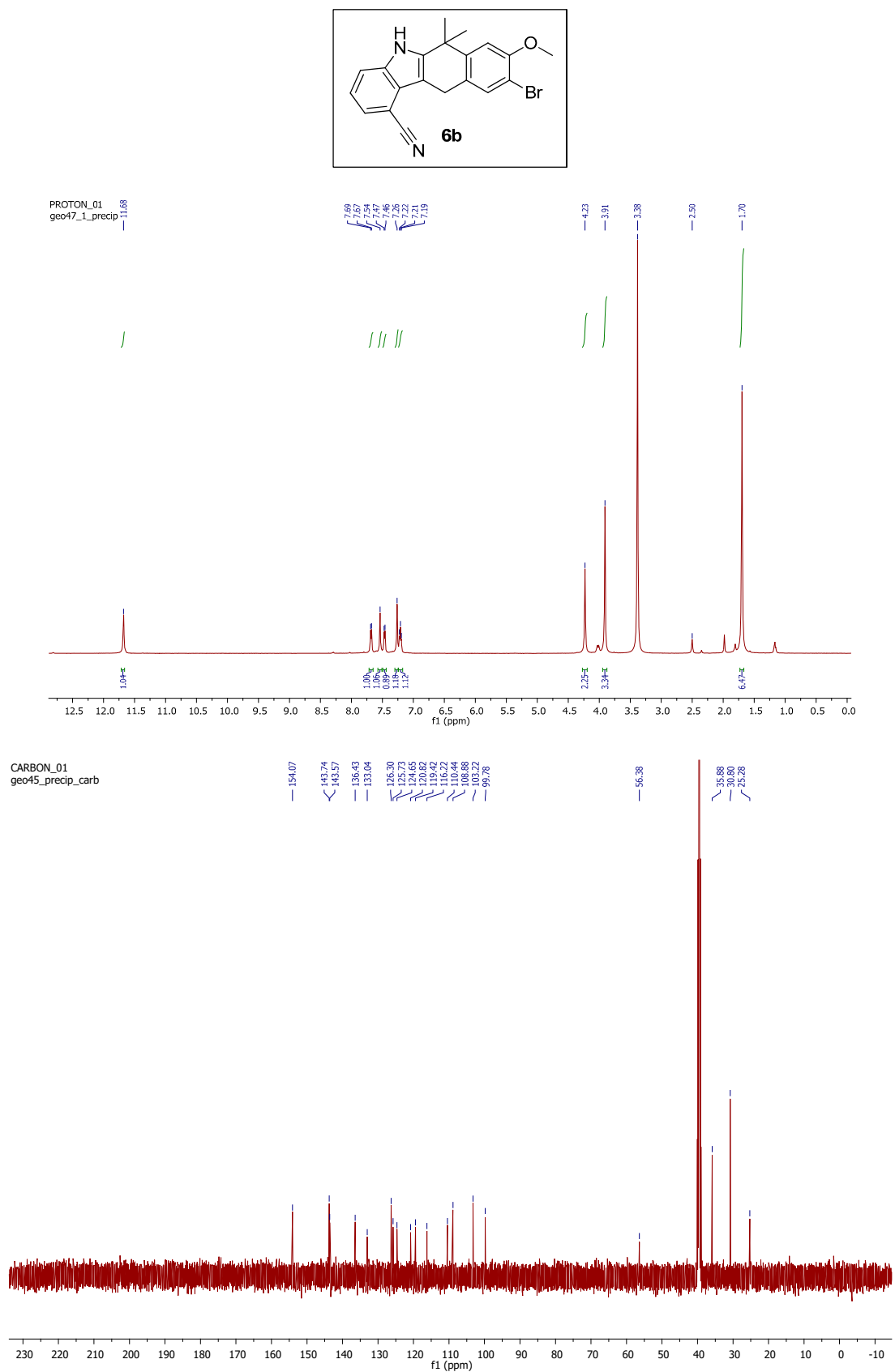


Figure S9. ^1H -NMR and ^{13}C -NMR spectra for compound **6b**

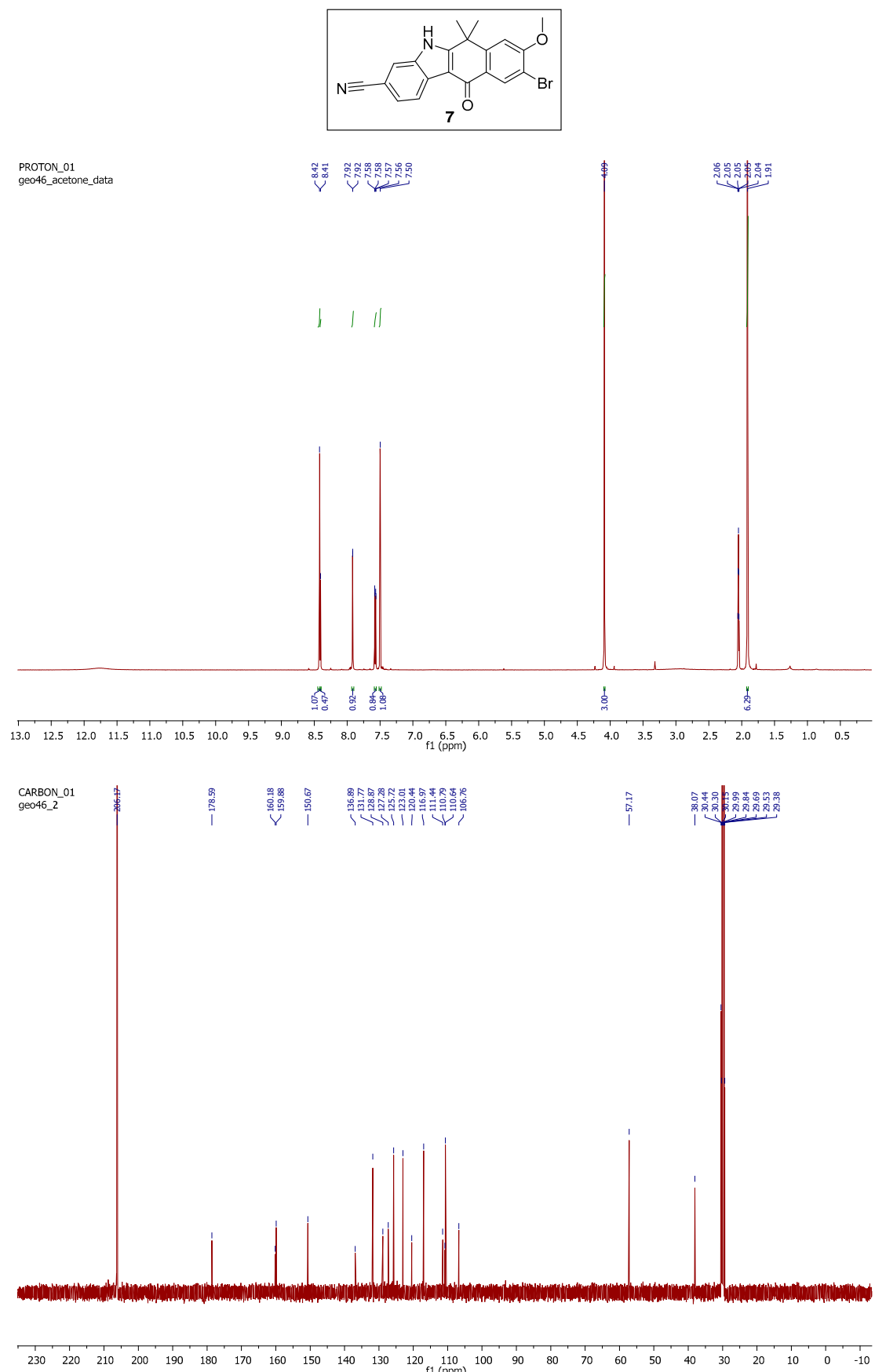
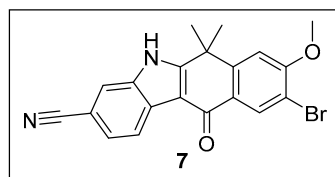


Figure S10. ^1H -NMR and ^{13}C -NMR spectra for compound **7**



Method 1

Retention time: 29.1 m

area: 80446192 (absorbance units x minutes)

total area: 80745691 (absorbance units x minutes)

area %: $(80446192 / 80745691) * 100 = 99.6\%$

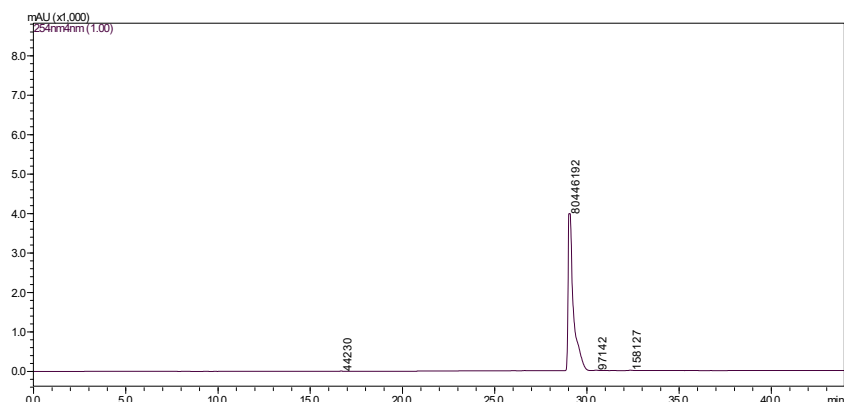


Figure S11. ESI-LCMS of compound 7 after column chromatography purification

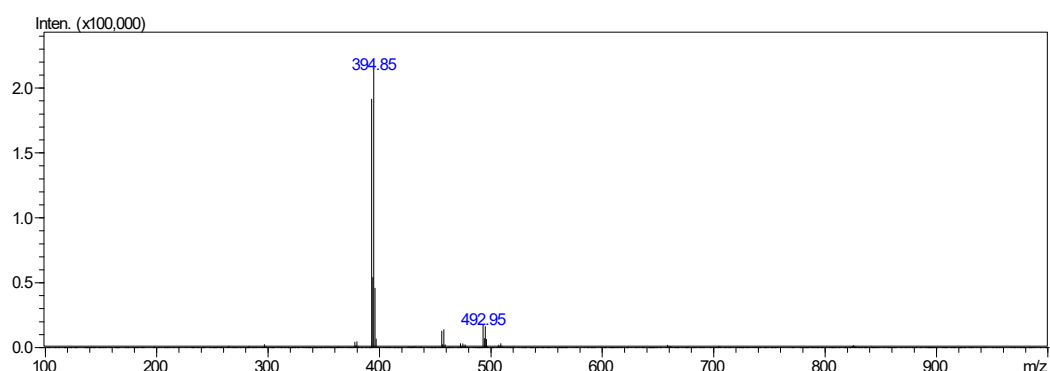


Figure S12. ESI-MS for 7, negative mode: m/z calcd mass for $C_{20}H_{14}BrN_2O_2 [M-H]^- = 393.02$, was found 394.85

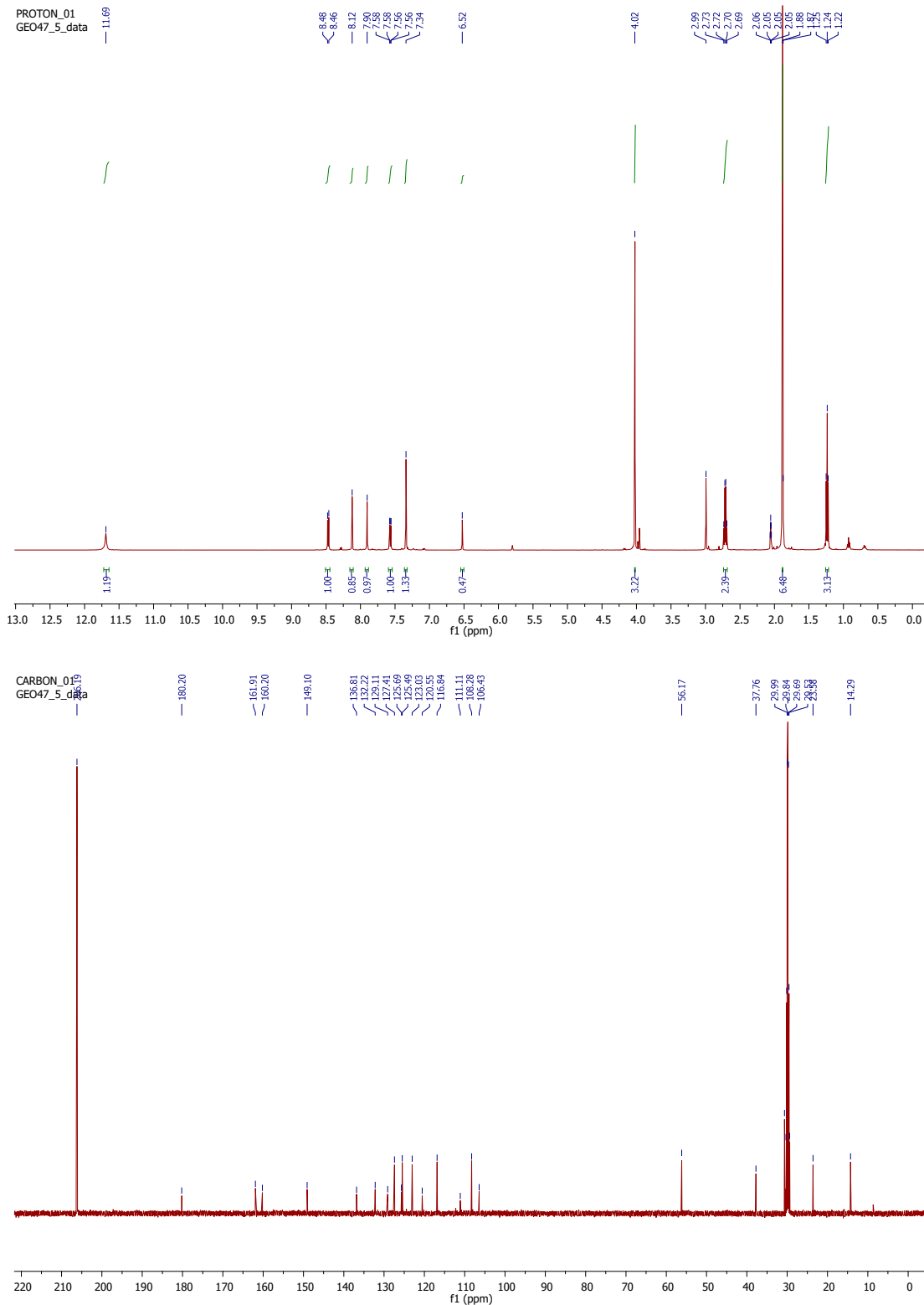
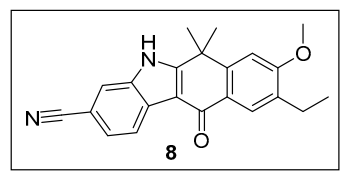
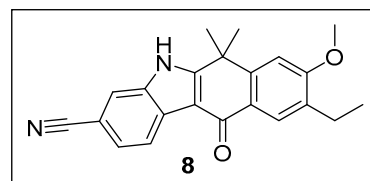


Figure S13. ¹H-NMR and ¹³C-NMR spectra for compound 8



Method 3

Retention time: 29.4 m

area: 31599537 (absorbance units x minutes)

total area: 34213713 (absorbance units x minutes)

area %: (31599537/34213713)*100 = 92.3 %

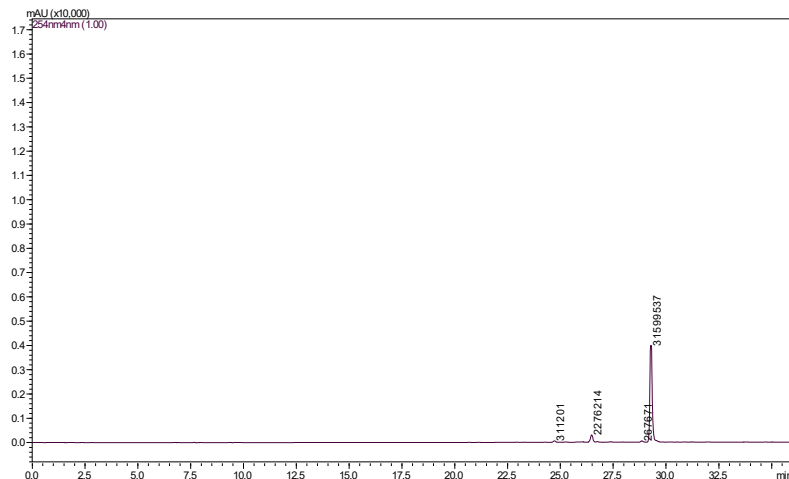


Figure S14. ESI-LCMS of compound **8** after column chromatography purification

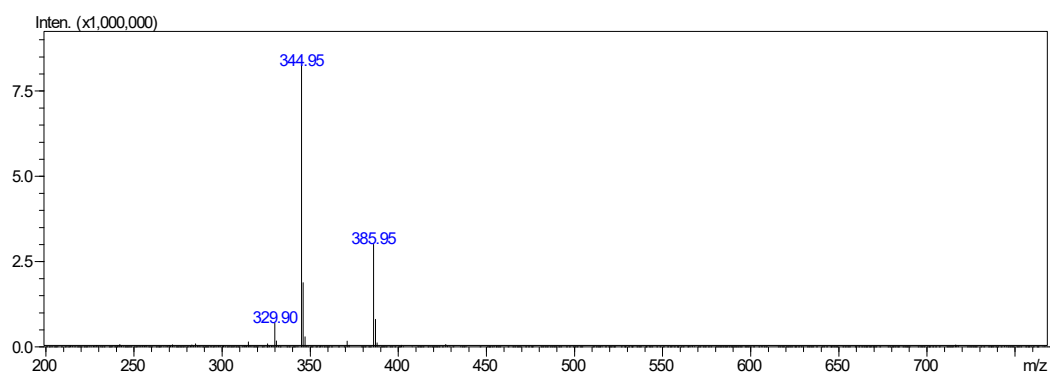


Figure S15. ESI-MS for **8**, positive mode: m/z calcd mass for C₂₂H₂₀N₂O₂ [M]⁺=344.15, was found 344.95

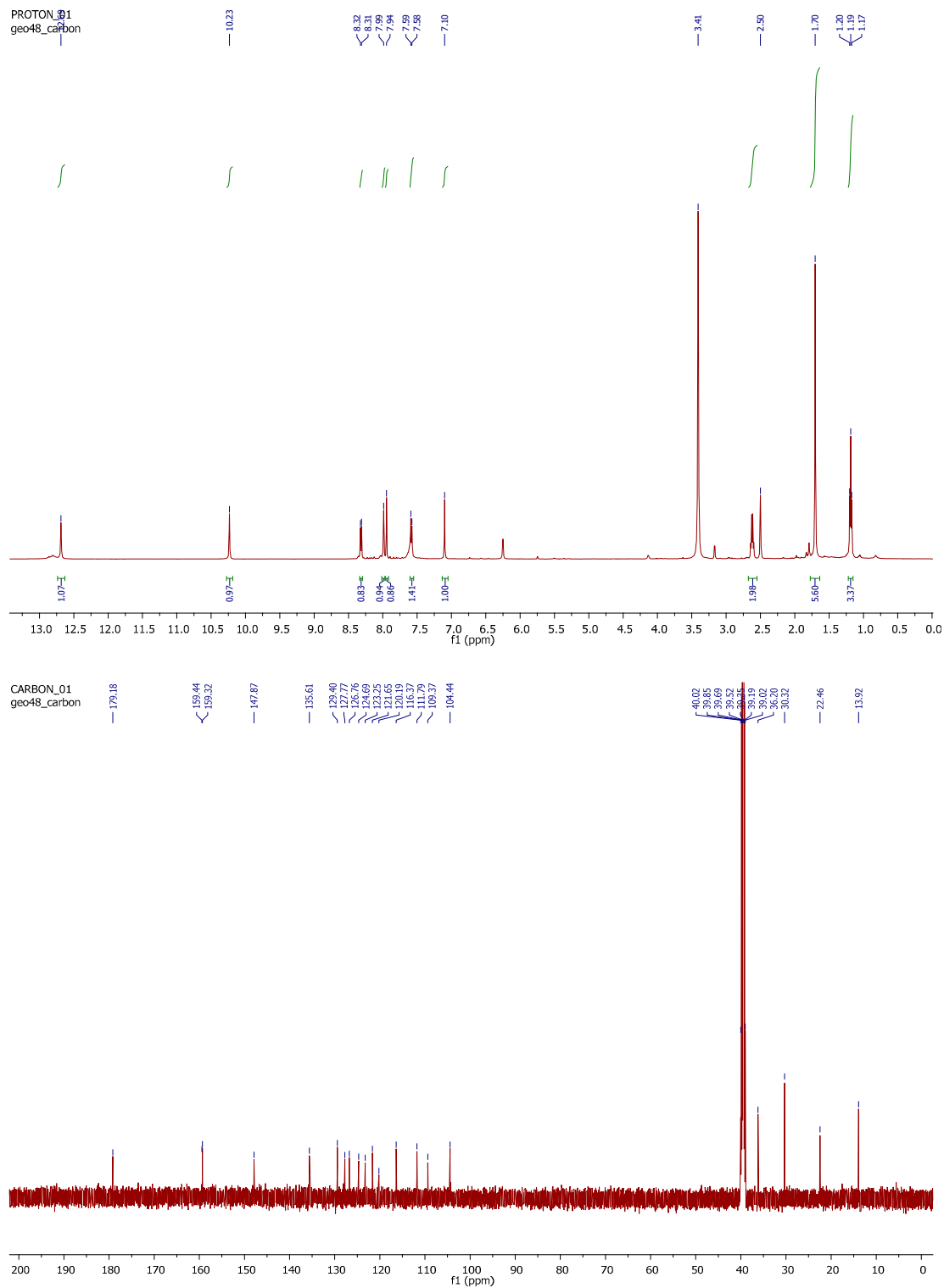
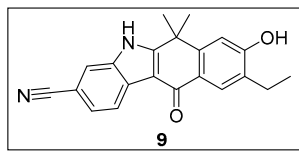
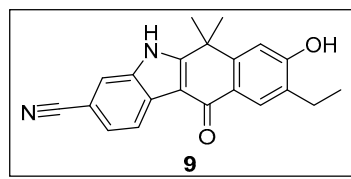


Figure S16. ¹H-NMR and ¹³C-NMR spectra for compound 9



MeOH isocratic elution

Retention time: 10.5 m

area: 93581467 (absorbance units x minutes)

total area: 93806687 (absorbance units x minutes)

area %: $(93581467 / 93806687) * 100 = 99.7 \%$

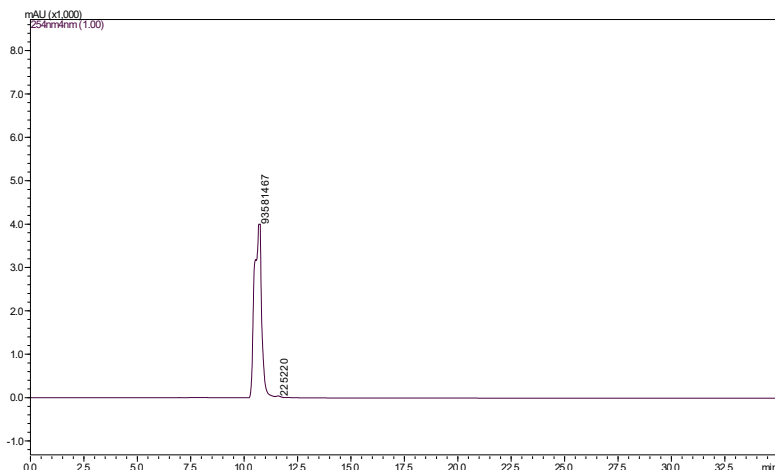


Figure S17. ESI-LCMS of compound **9** after column chromatography purification

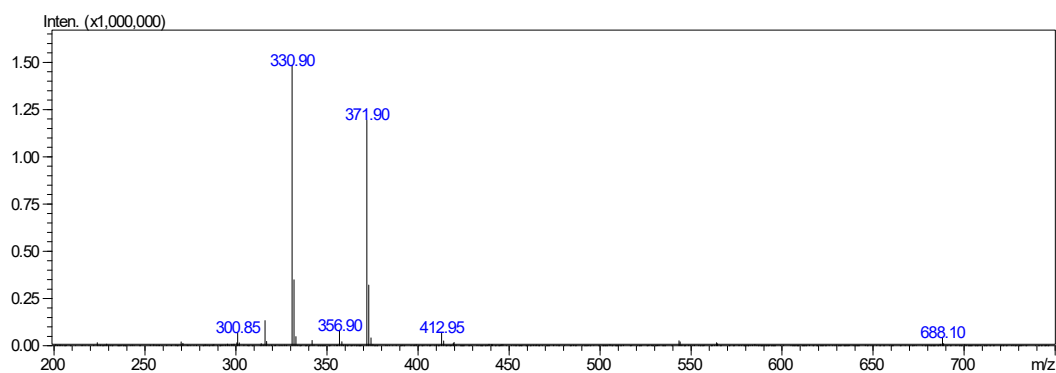


Figure S18. ESI-MS for **9**, positive mode: m/z calcd mass for $C_{21}H_{18}N_2O_2 [M+H]^+$ = 330.14, was found 330.90

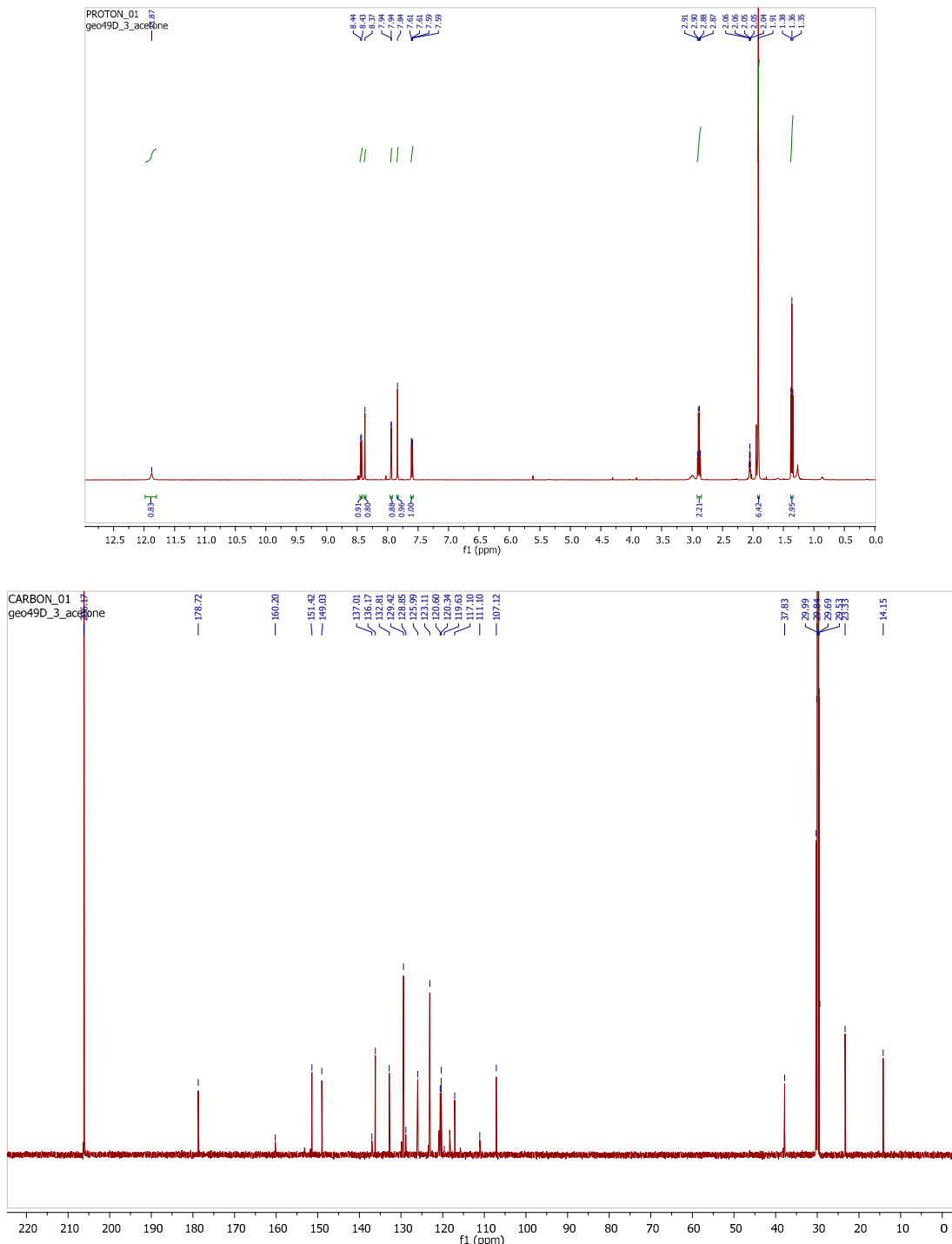
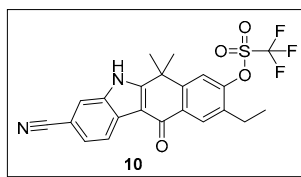
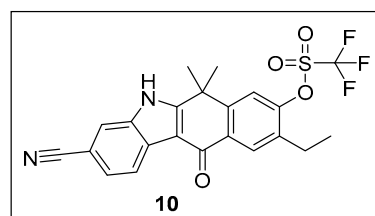


Figure S19. ¹H-NMR and ¹³C-NMR spectra for compound 10



Method 1

Retention time: 32.1 m

area: 28426895 (absorbance units x minutes)

total area: 29099709 (absorbance units x minutes)

area %: (28426895/29099709)*100 = 97.7 %

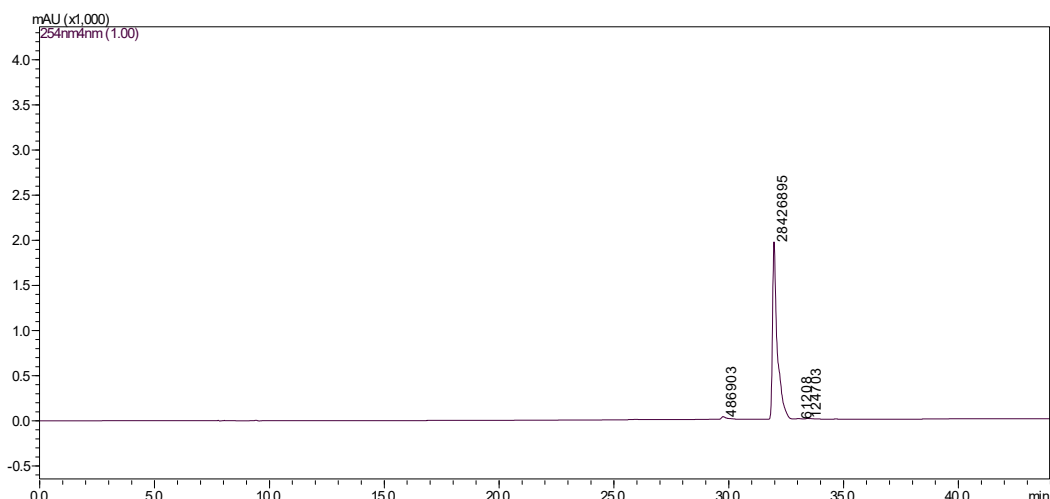


Figure S20. ESI-LCMS of compound **10** after column chromatography purification

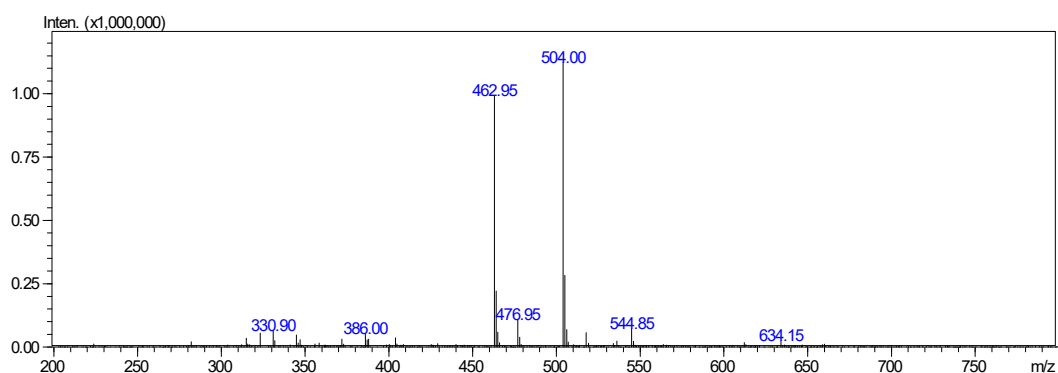


Figure S21. ESI-MS for **10**, positive mode: m/z calcd mass for C₂₂H₁₇F₃N₂O₄S [M]⁺=462.08, was found 462.95

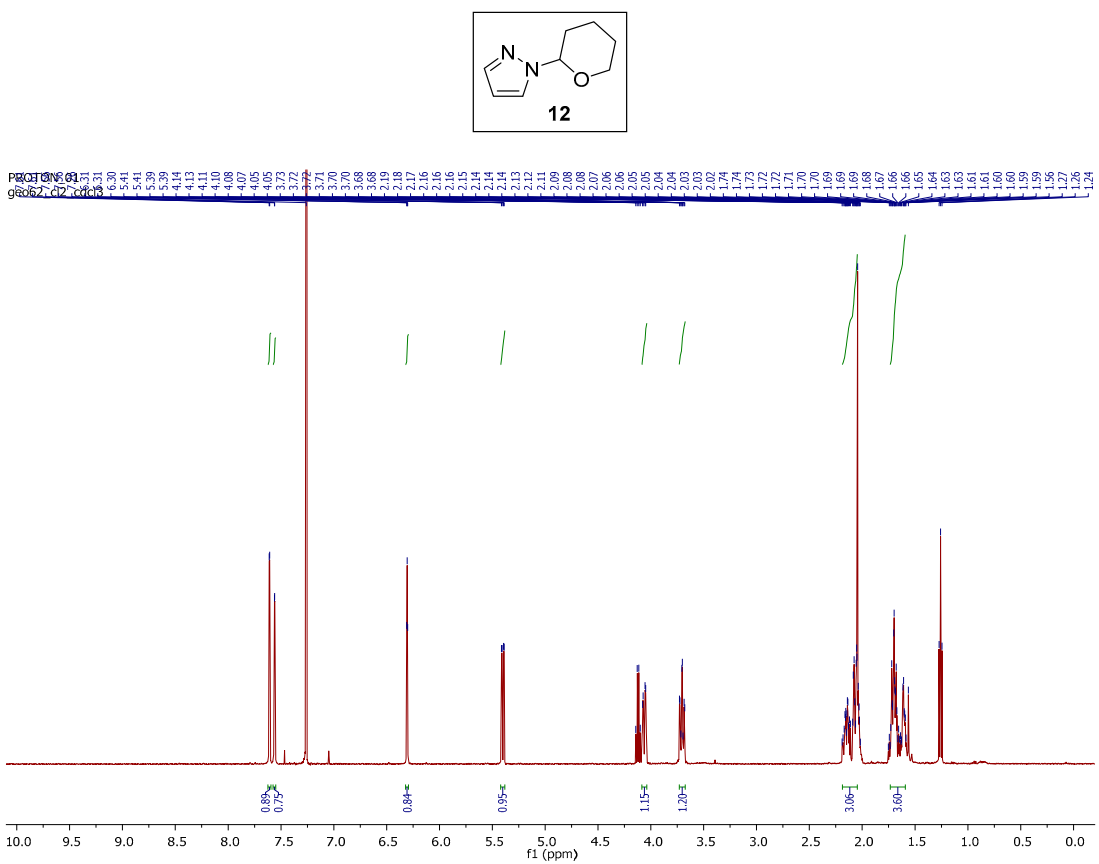


Figure S22. ^1H -NMR for compound **12**

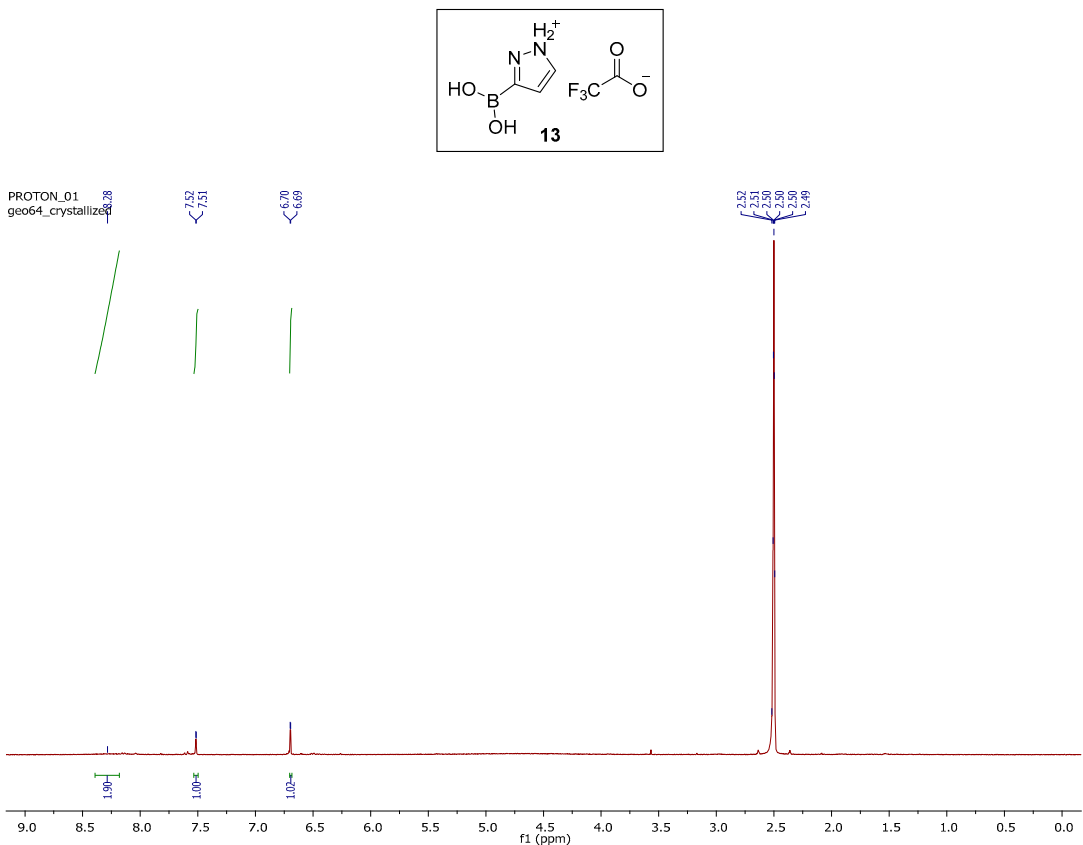


Figure S23. ^1H -NMR for compound **13**

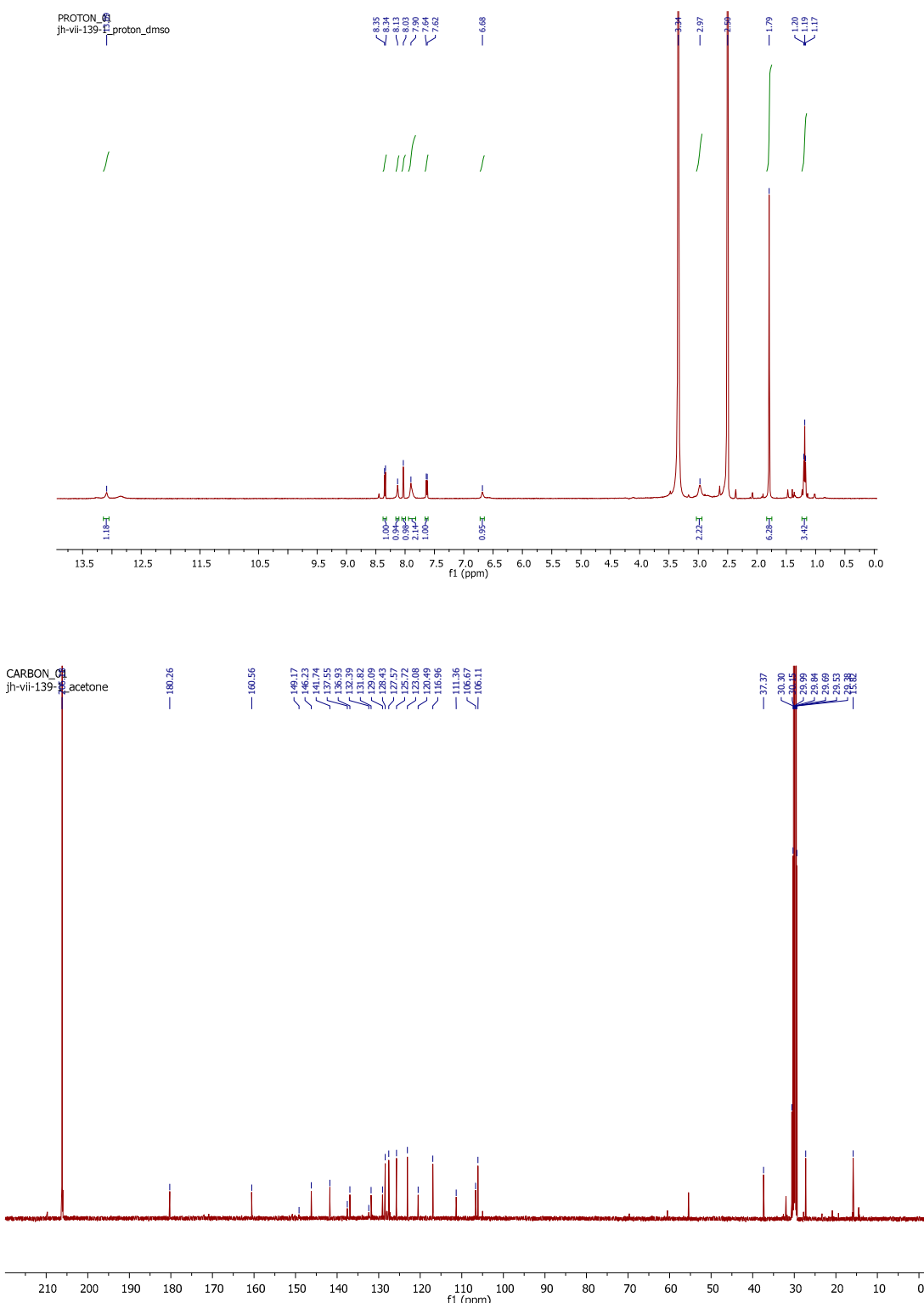
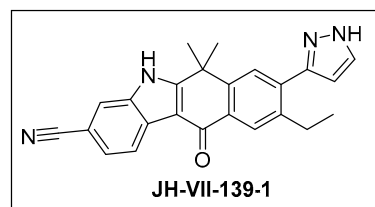
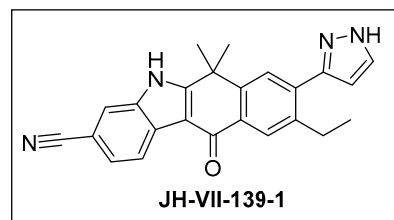


Figure S24. ¹H-NMR and ¹³C-NMR spectra for compound JH-VII-139-1



Method 1

Retention time: 26.3 m

area: 8070456 (absorbance units x minutes)

total area: 8258696 (absorbance units x minutes)

area %: $(8070456/8258696)*100 = 97.7 \%$

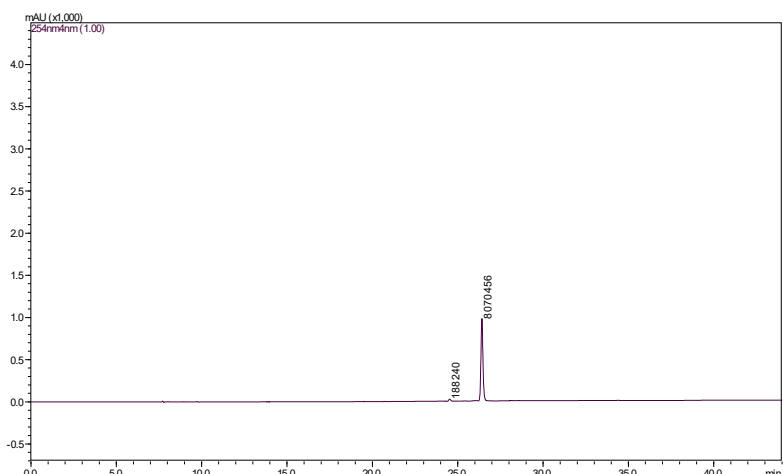


Figure S25. ESI-LCMS of compound JH-VII-139-1 after column chromatography purification

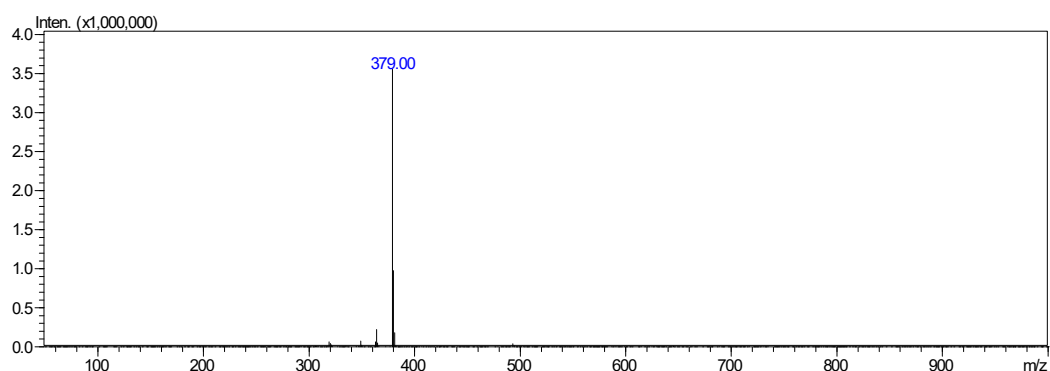


Figure S26. ESI-MS for JH-VII-139-1, negative mode: m/z calcd mass for $C_{24}H_{20}N_4O [M-H]^- = 379.16$, was found 379.00

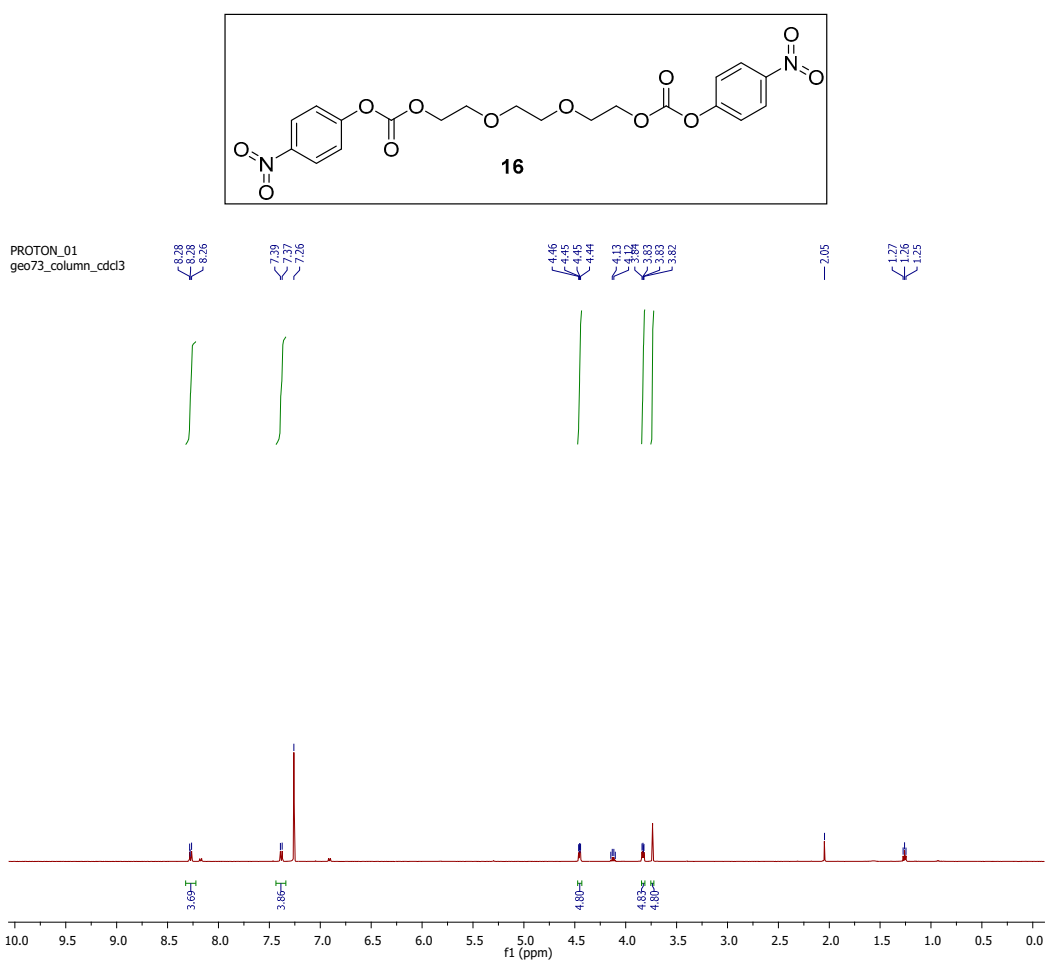


Figure S27. ^1H -NMR spectrum for compound **16**

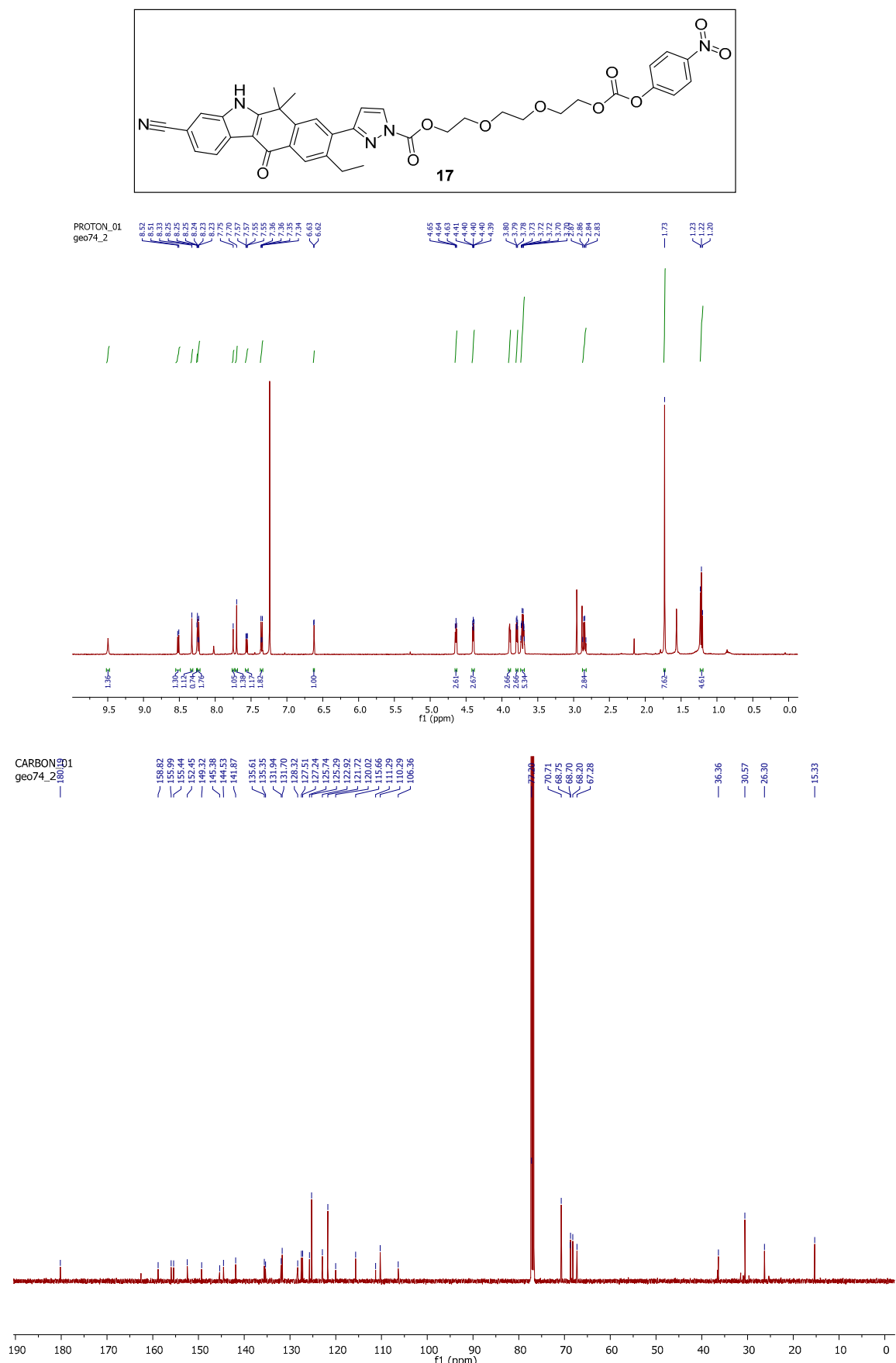
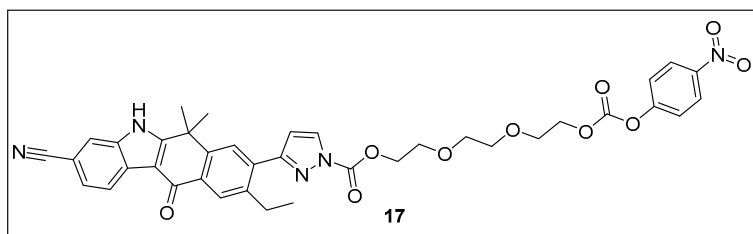


Figure S28. ¹H-NMR and ¹³C-NMR spectra for compound **17**



Method 1

Retention time: 29.5 m

area: 25509809 (absorbance units x minutes)

total area: 26264849 (absorbance units x minutes)

area %: (25509809/26264849)*100 = 97.1 %

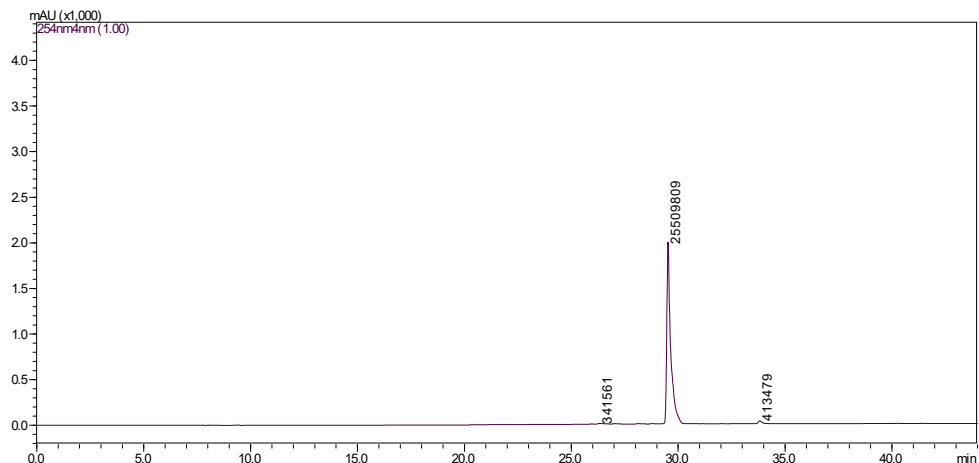


Figure S29. ESI-LCMS of compound **17** after column chromatography purification

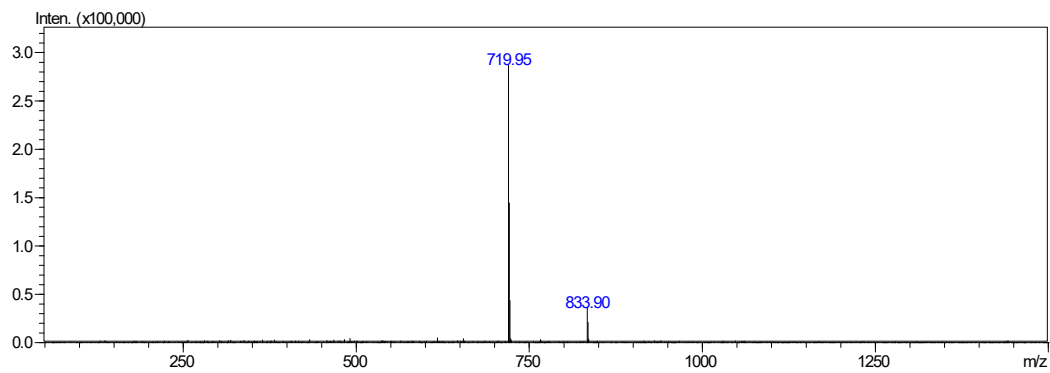


Figure S30. ESI-MS for **17**, negative mode: m/z calcd mass for $C_{38}H_{35}N_5O_{10}$ $[M+H]^+$ =720.24, was found 719.95

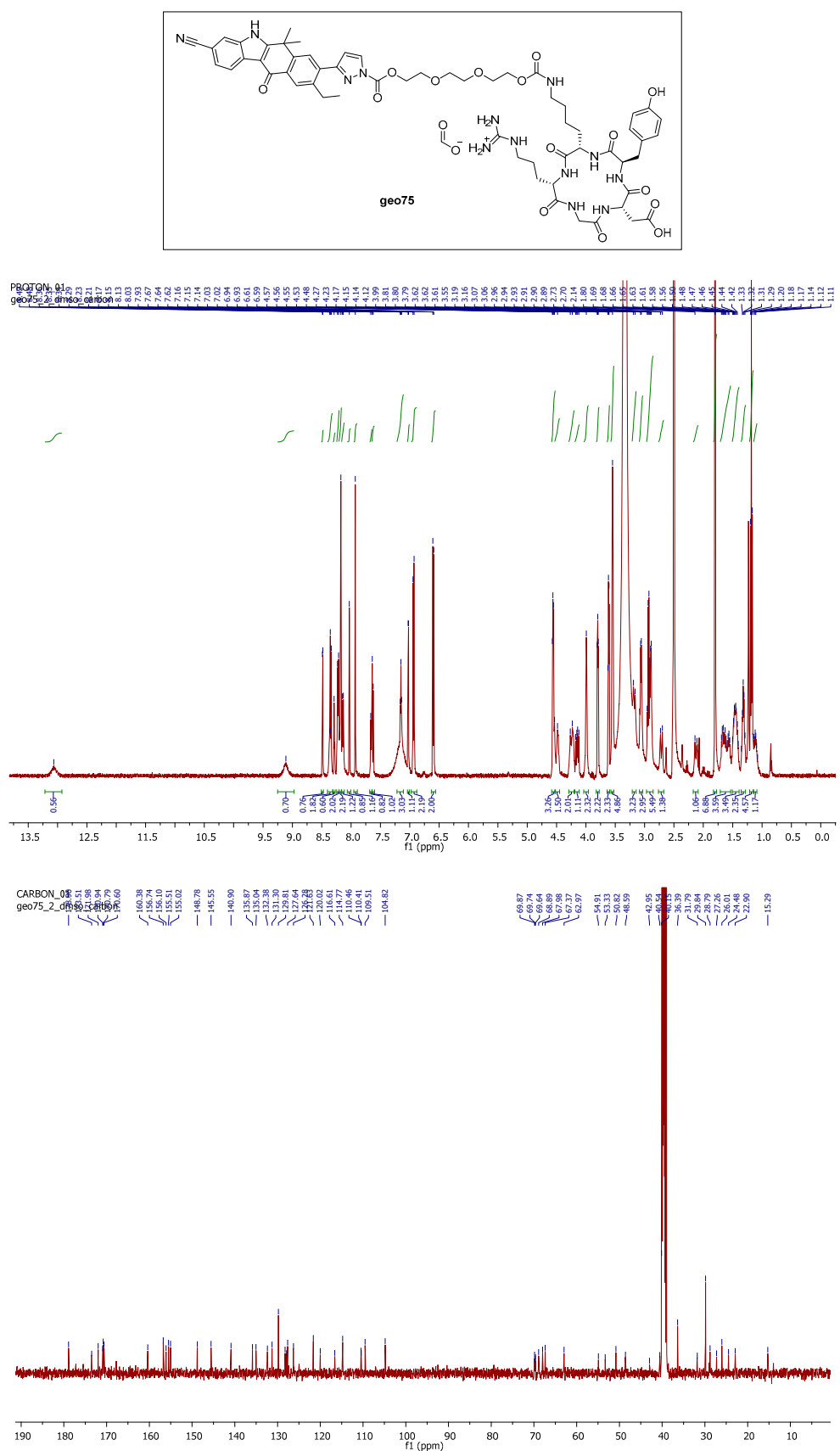
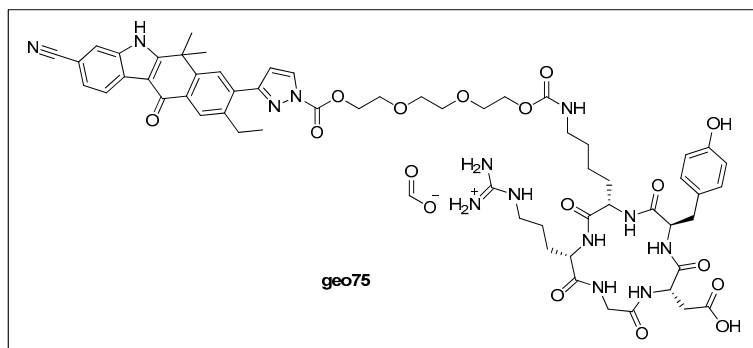


Figure S31. ^1H -NMR and ^{13}C -NMR spectra for compound geo75



Method 1

Retention time: 20.9 m

area: 32830161 (absorbance units x minutes)

total area: 33143414 (absorbance units x minutes)

area %: (32830161/33143414)*100 = 99.0 %

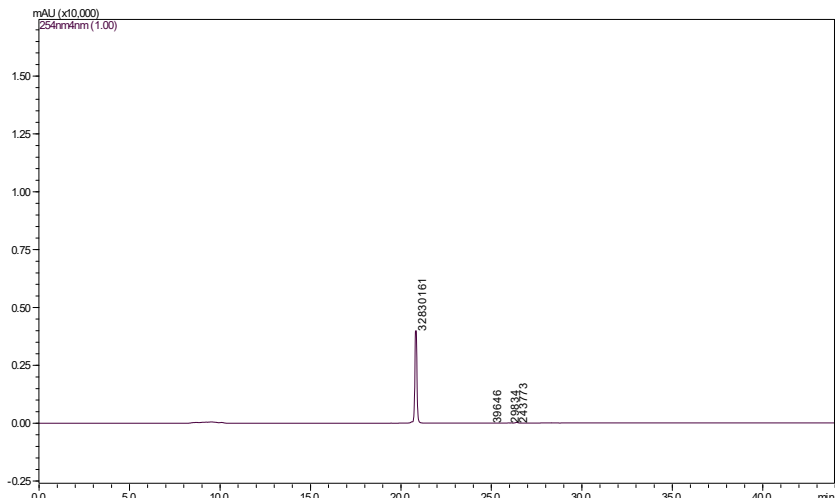


Figure S32. ESI-LCMS of compound geo75 after column chromatography purification

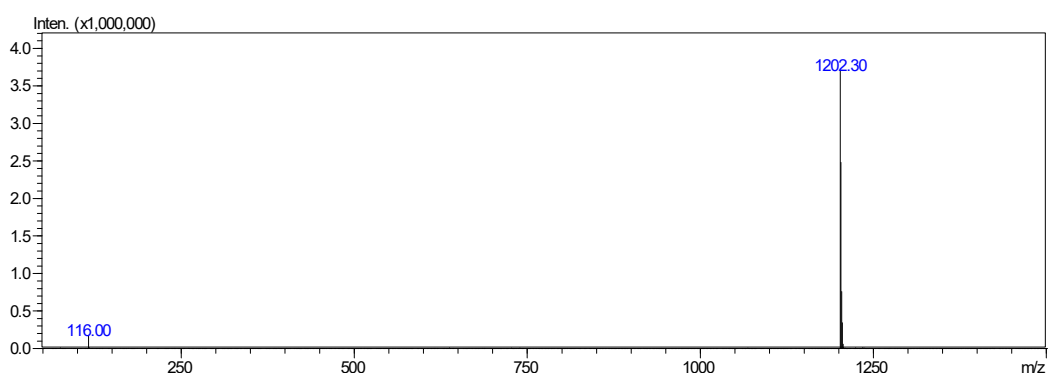


Figure S33. ESI-MS for geo75, positive mode: m/z calcd mass for C₅₉H₇₁N₁₃O₁₅ [M+H]⁺=1202.52, was found 1202.30.

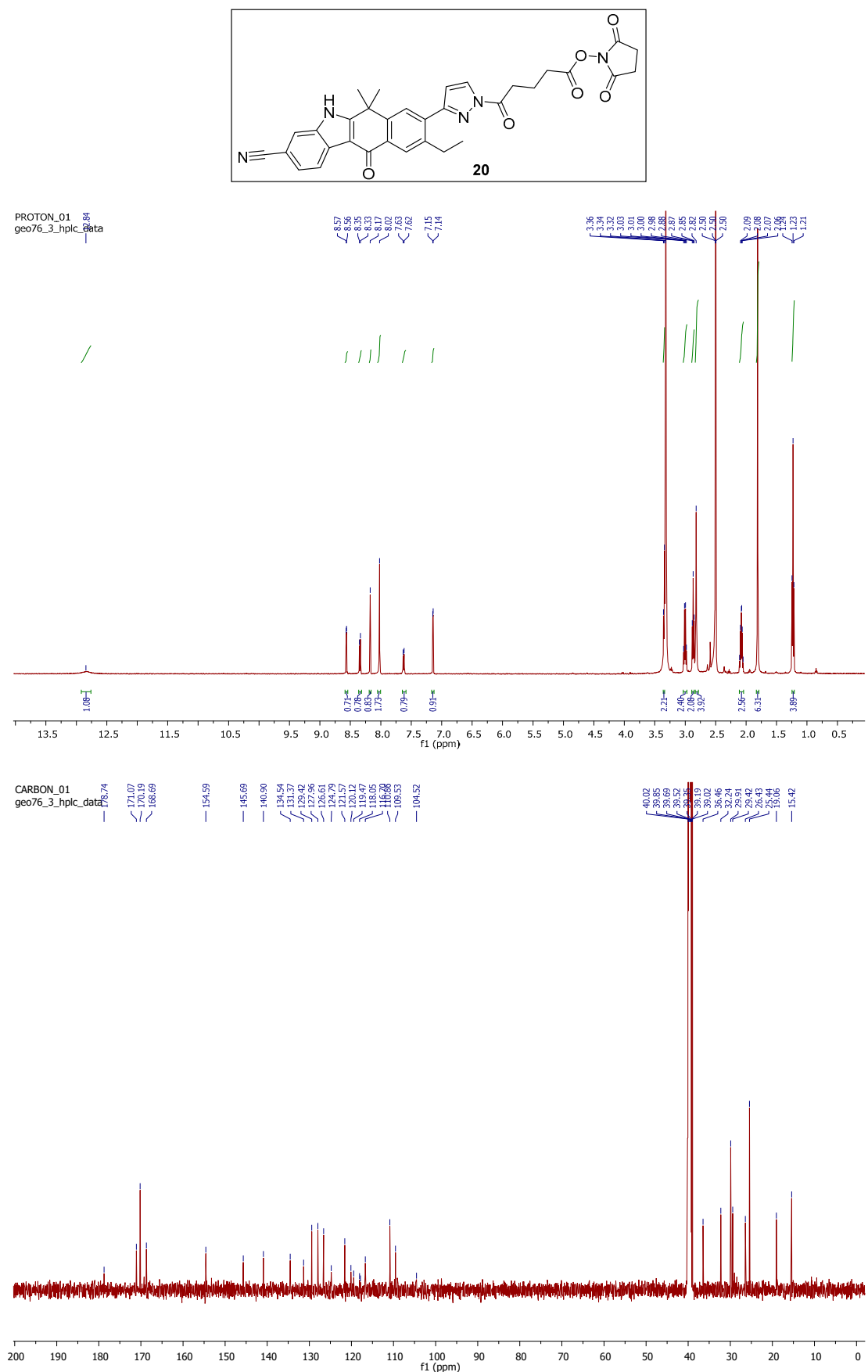
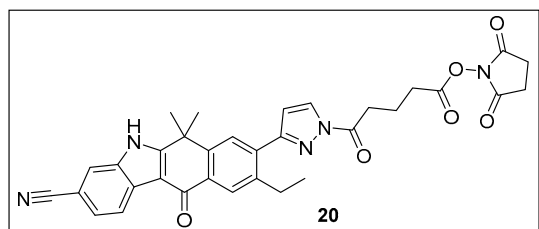


Figure S34. ^1H -NMR and ^{13}C -NMR spectra for compound **20**



Method 1

Retention time: 28.9 m

area: 7423047 (absorbance units x minutes)

total area: 8244264 (absorbance units x minutes)

area %: $(7423047/8244264) * 100 = 90.1 \%$

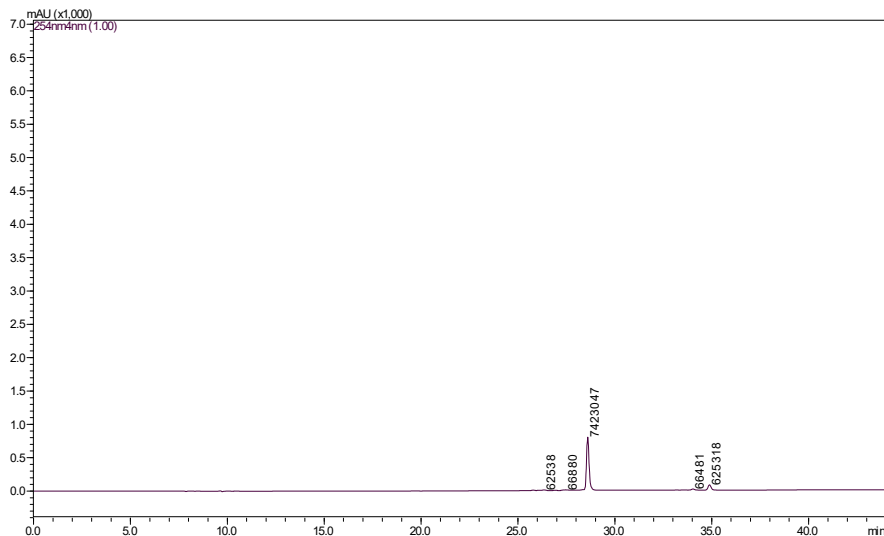


Figure S35. ESI-LCMS of compound **20** after column chromatography purification

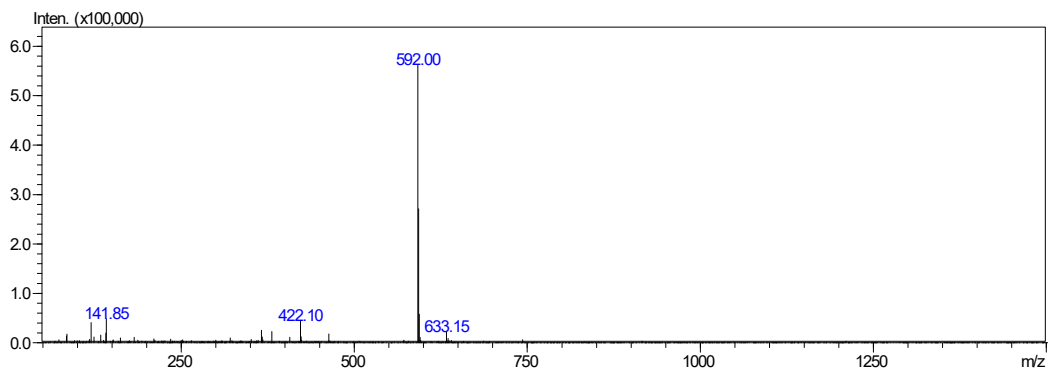


Figure S36. ESI-MS for **20**, positive mode: m/z calcd mass for $C_{33}H_{29}N_5O_6 [M+H]^+$ = 592.21, was found 592.00

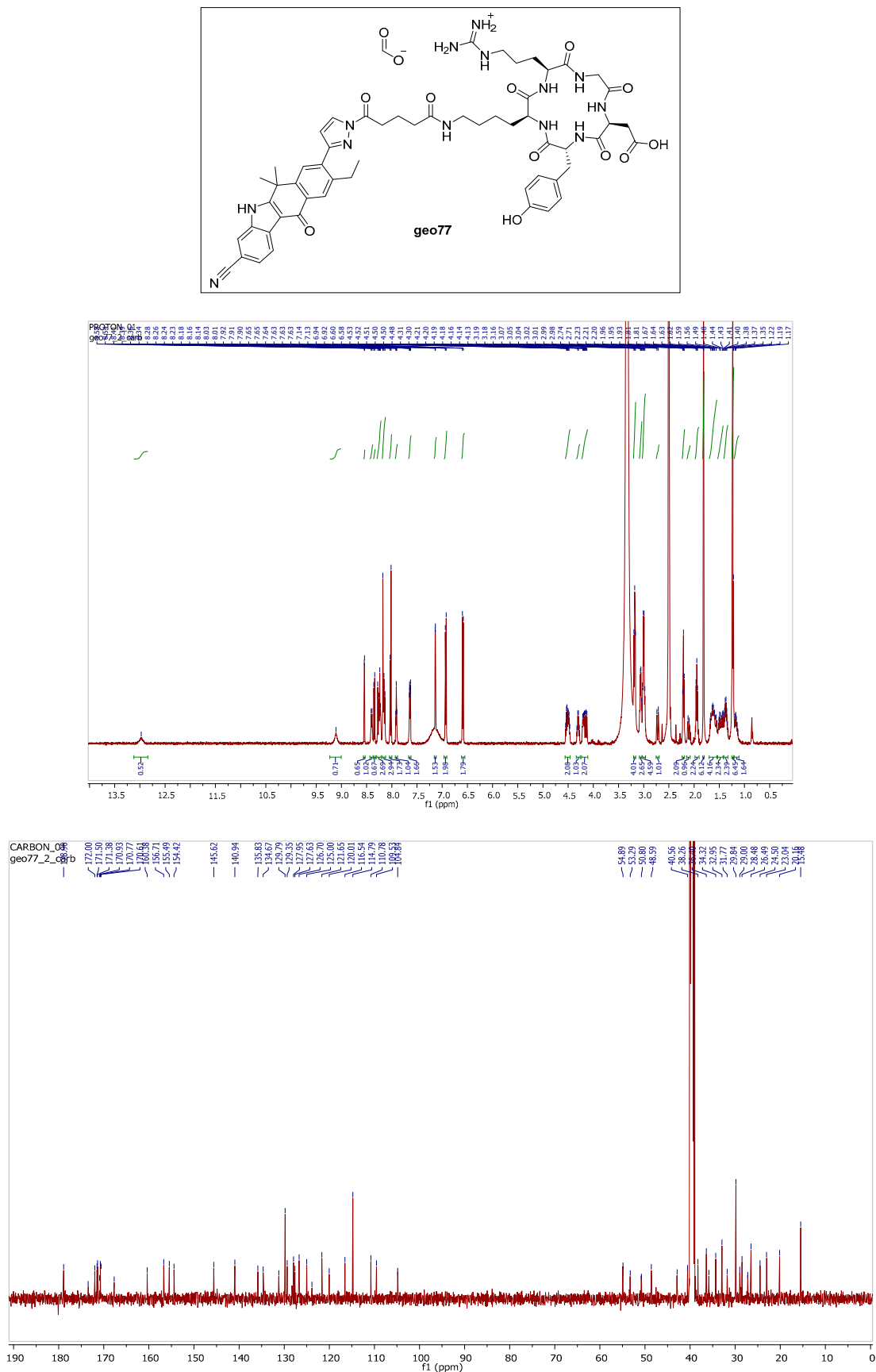
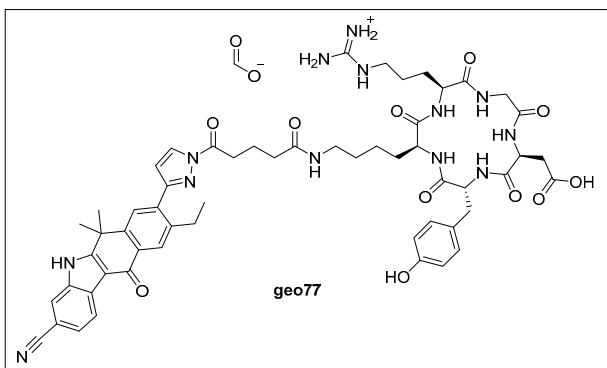


Figure S37. ^1H -NMR and ^{13}C -NMR spectra for compound geo77.



Method 1

Retention time: 20.9 m

area: 54752812 (absorbance units x minutes)

total area: 55219719 (absorbance units x minutes)

area %: $(54752812/55219719) * 100 = 99.1 \%$

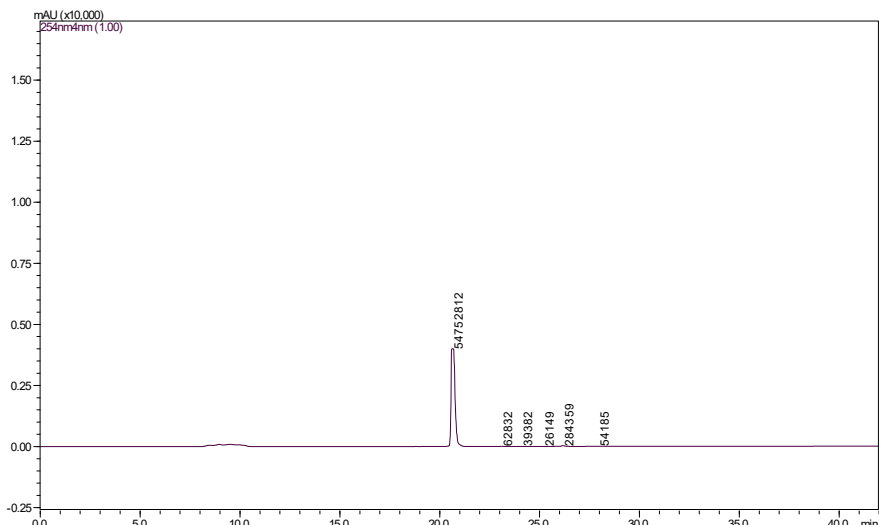


Figure S38. ESI-LCMS of compound geo77 after HPLC purification.

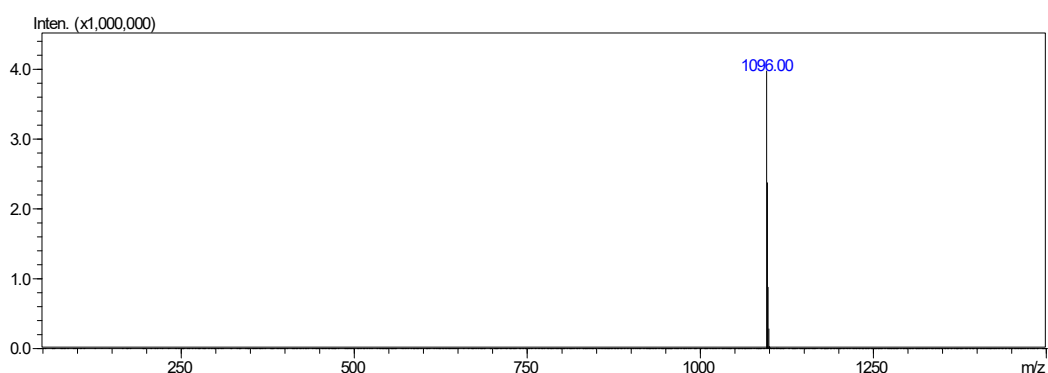


Figure S39. ESI-MS for geo77, positive mode: m/z calcd mass for $\text{C}_{56}\text{H}_{66}\text{N}_{13}\text{O}_{11}$ $[\text{M}+\text{H}]^+ = 1096.49$, was found 1096.00.

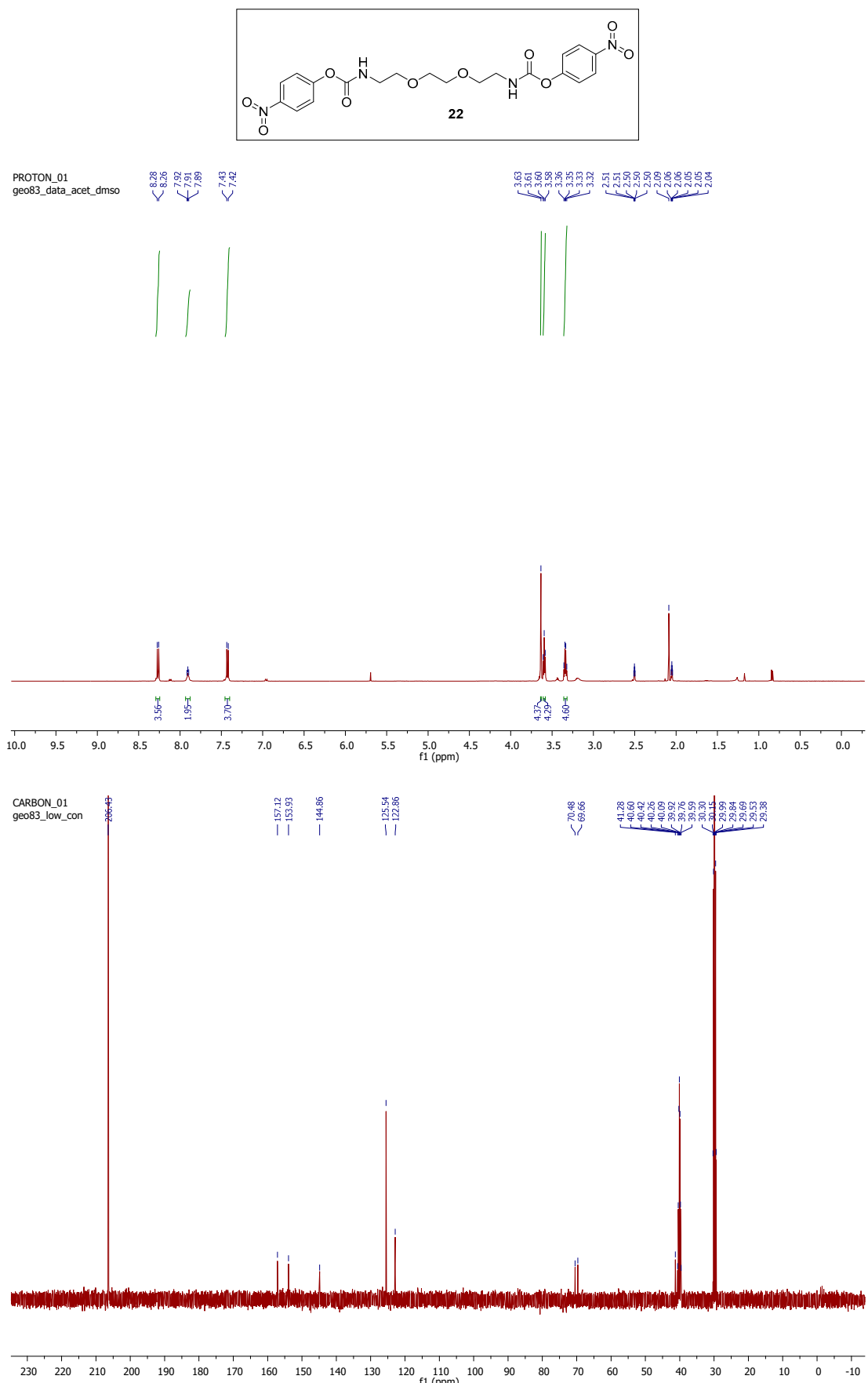


Figure S40. ^1H -NMR and ^{13}C -NMR spectra for compound **22**.

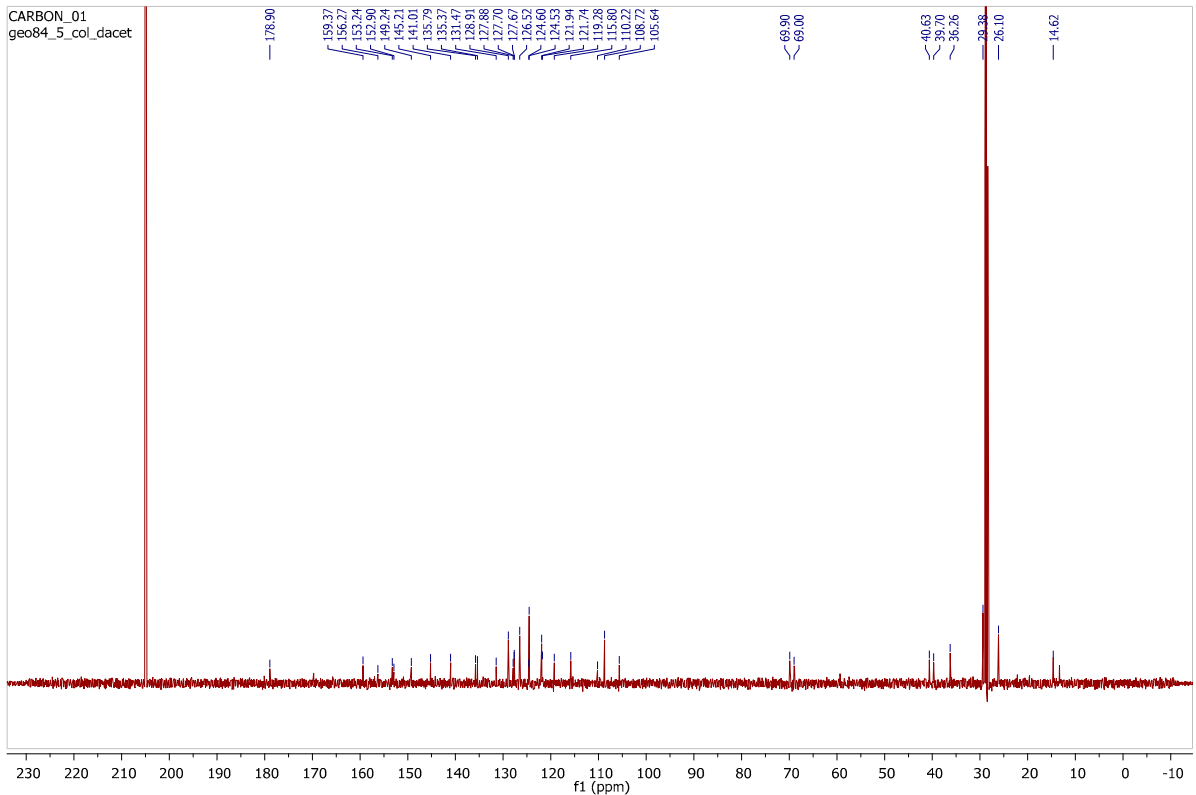
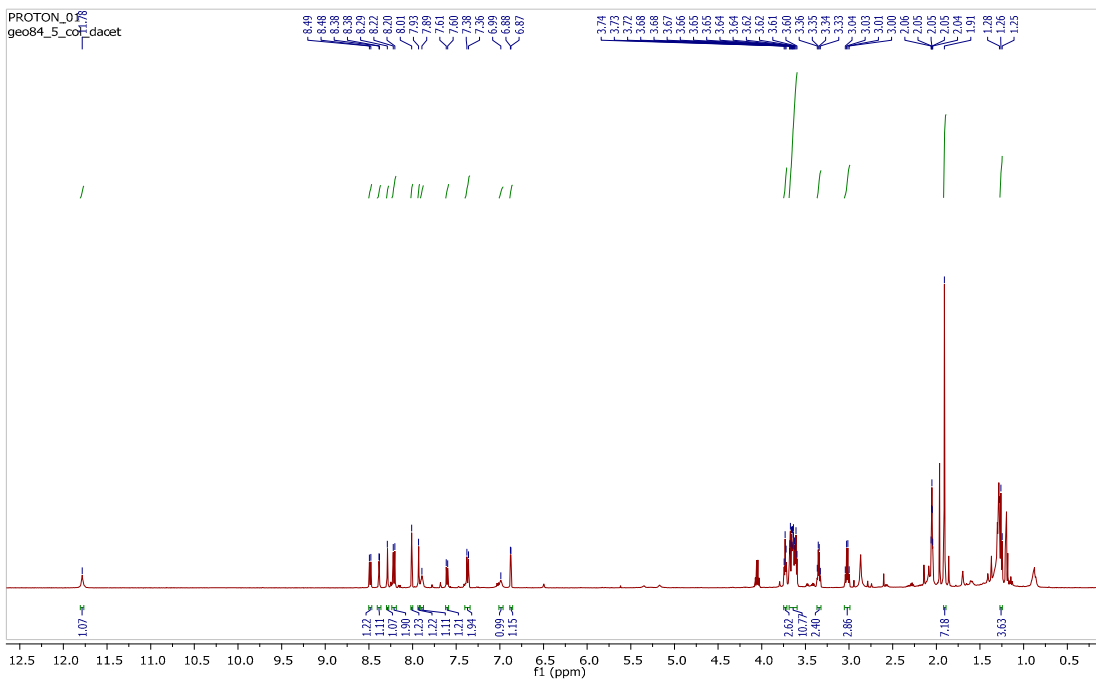
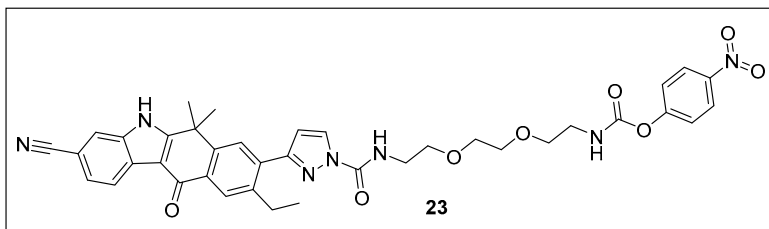


Figure S41. ¹H-NMR and ¹³C-NMR spectra for compound 23.

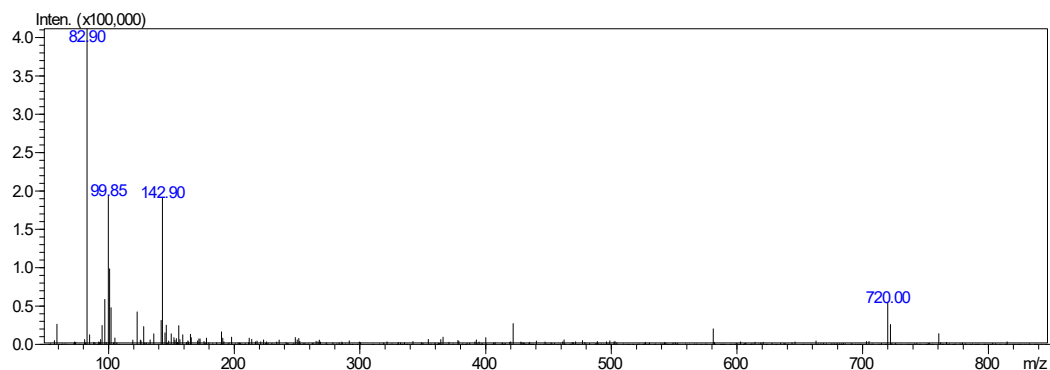
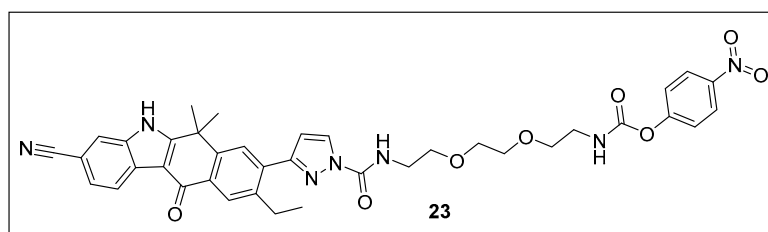
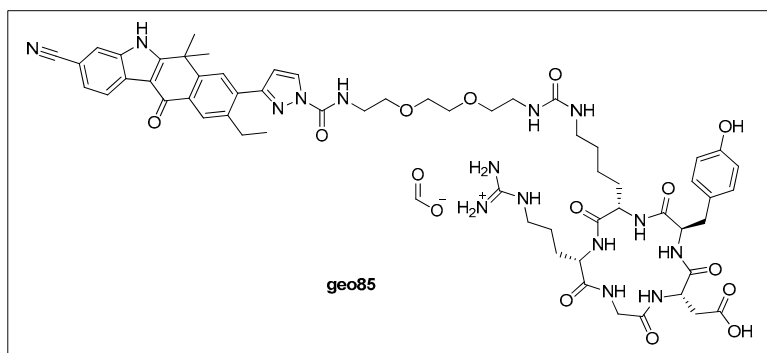


Figure S42. ESI-MS for **23**, positive mode: m/z calcd mass for $C_{38}H_{38}N_7O_8 [M+H]^+$ =720.27, was found 720.00



Method 1

Retention time: 20.9 m

area: 11577332 (absorbance units x minutes)

total area: 11811289 (absorbance units x minutes)

area %: $(11577332 / 11811289) * 100 = 98.0 \%$

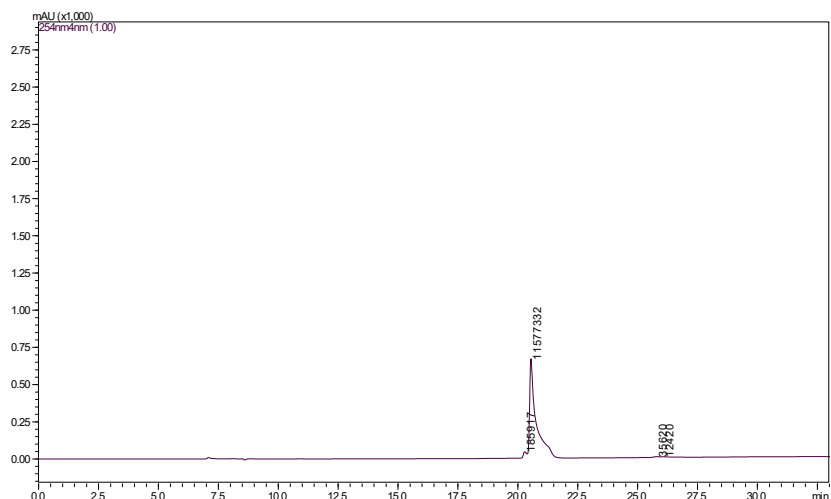


Figure S43. ESI-LCMS of compound geo85 after HPLC purification

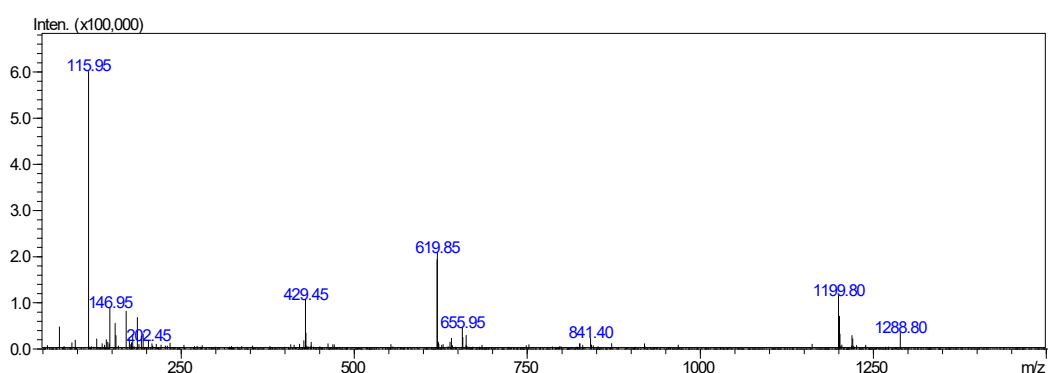


Figure S44. ESI-MS for geo85, positive mode: m/z calcd mass for $C_{59}H_{74}N_{15}O_{13}$ $[M+H]^+=1200.55$, was found 1199.80.

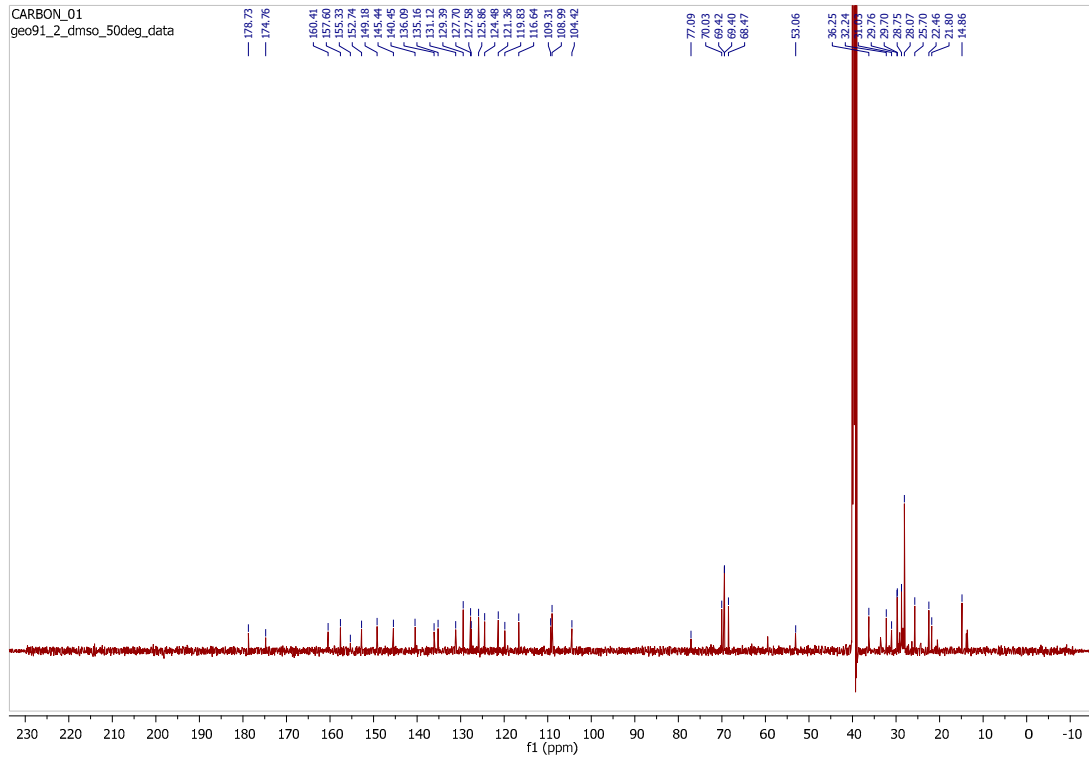
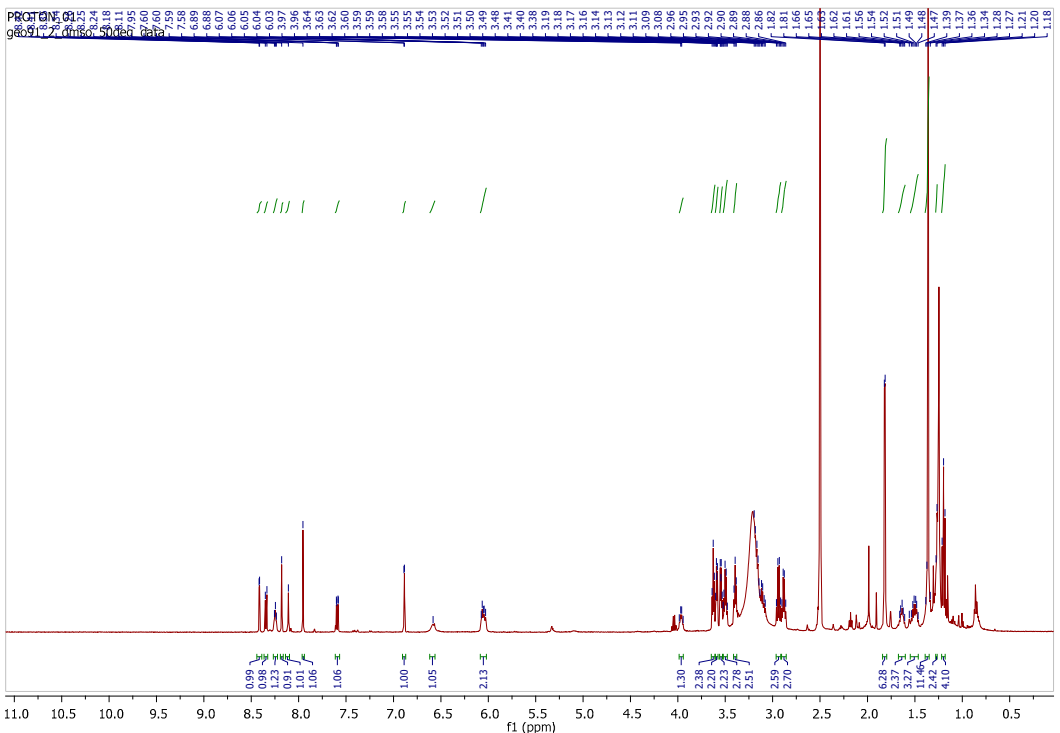
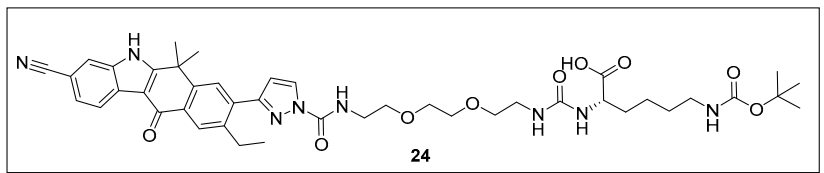
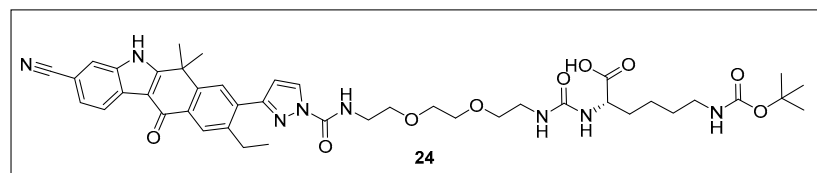


Figure S45. ¹H-NMR and ¹³C-NMR spectra for compound 24.



Method 1

Retention time: 27.4 m

area: 6702040 (absorbance units x minutes)

total area: 7142814 (absorbance units x minutes)

area %: $(6702040/7142814) * 100 = 93.8 \%$

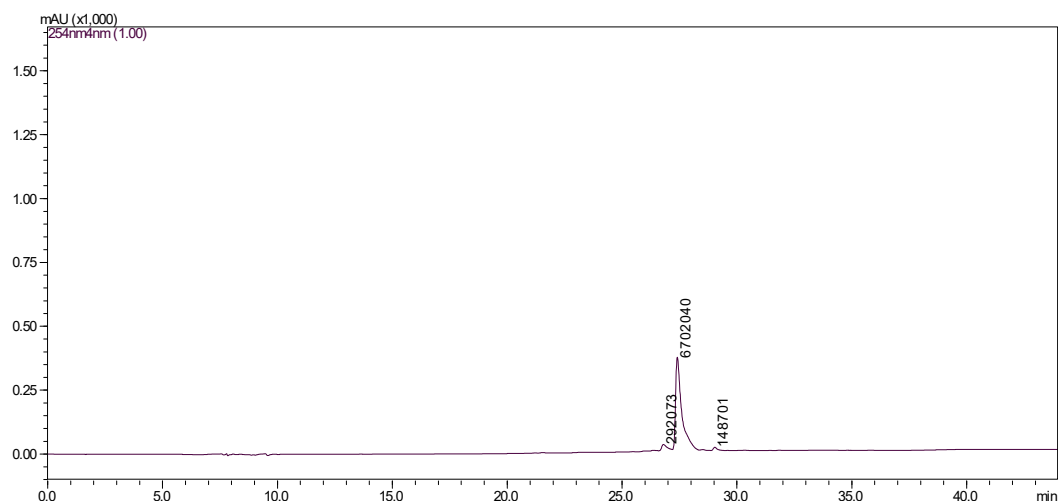


Figure S46. ESI-LCMS of compound **24** after column chromatography purification

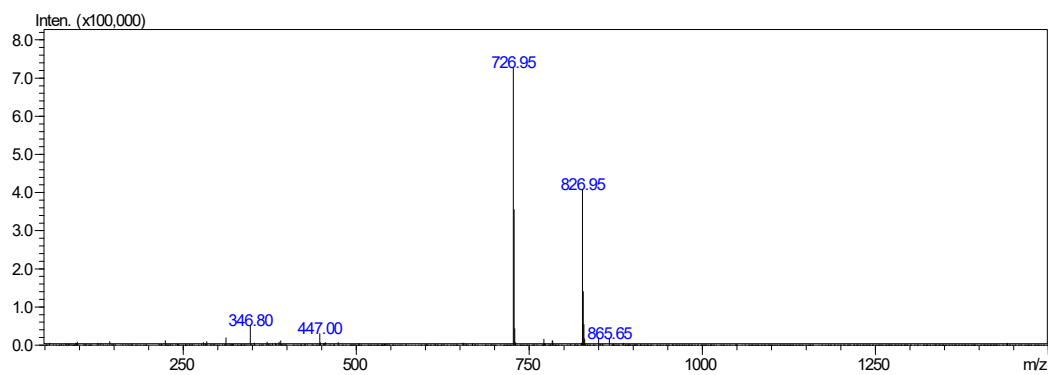


Figure S47. ESI-MS for **24**, positive mode: m/z calcd mass for $C_{43}H_{55}N_8O_9 [M+H]^+$ = 827.40, was found 826.95

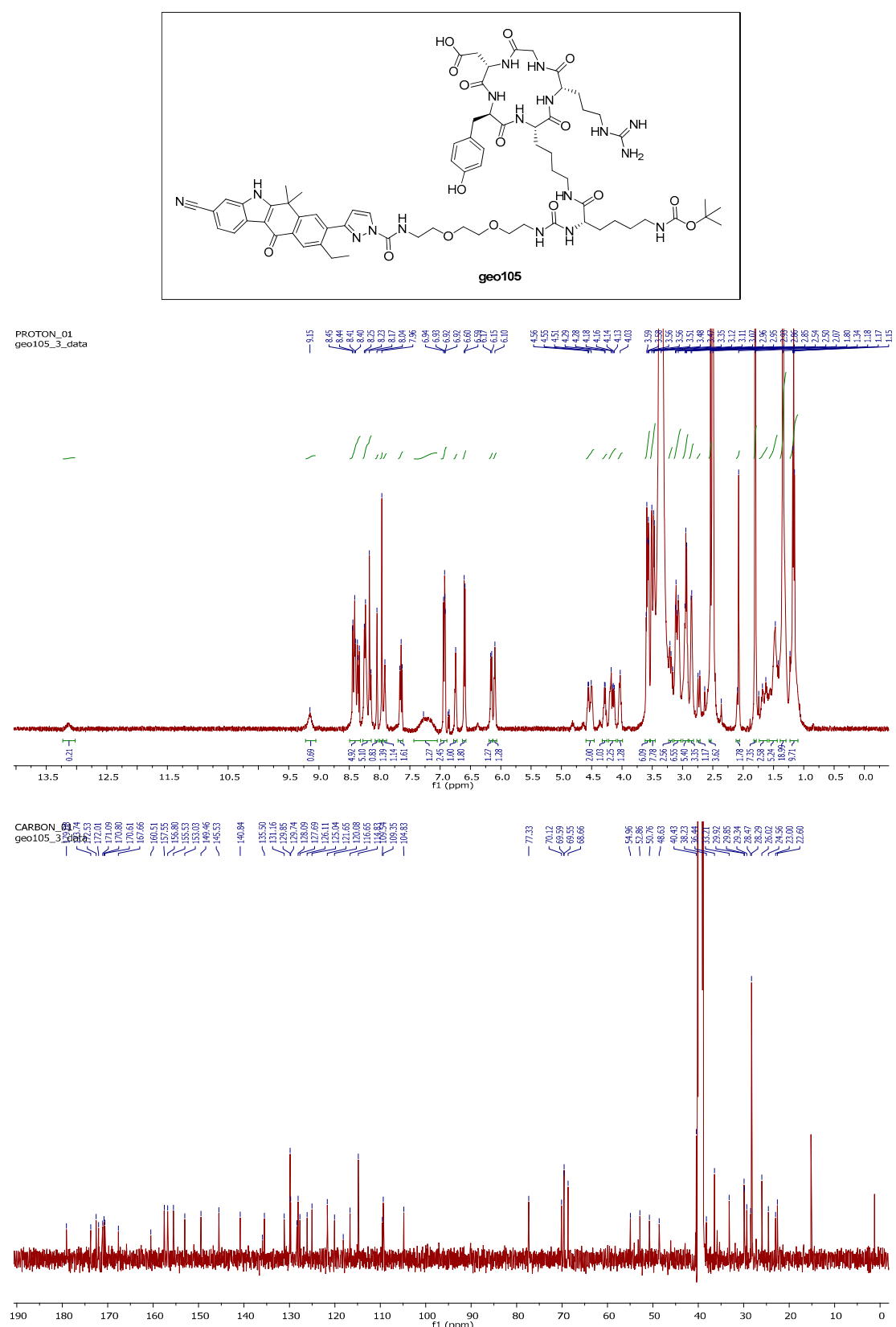
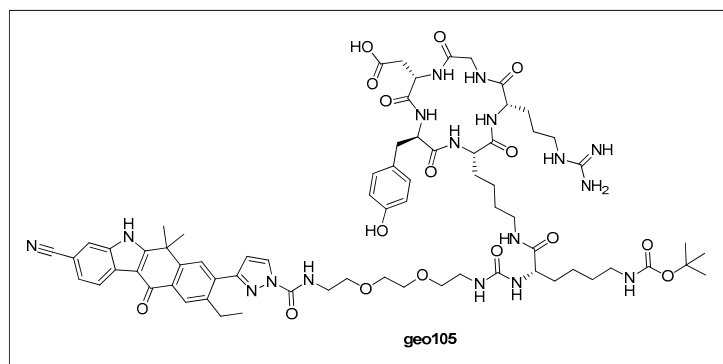


Figure S48. ¹H-NMR and ¹³C-NMR spectra for compound geo105.



Method 1

Retention time: 21.8 m

area: 11056999 (absorbance units x minutes)

total area: 11122330 (absorbance units x minutes)

area %: $(11056999/11122330) * 100 = 99.4 \%$

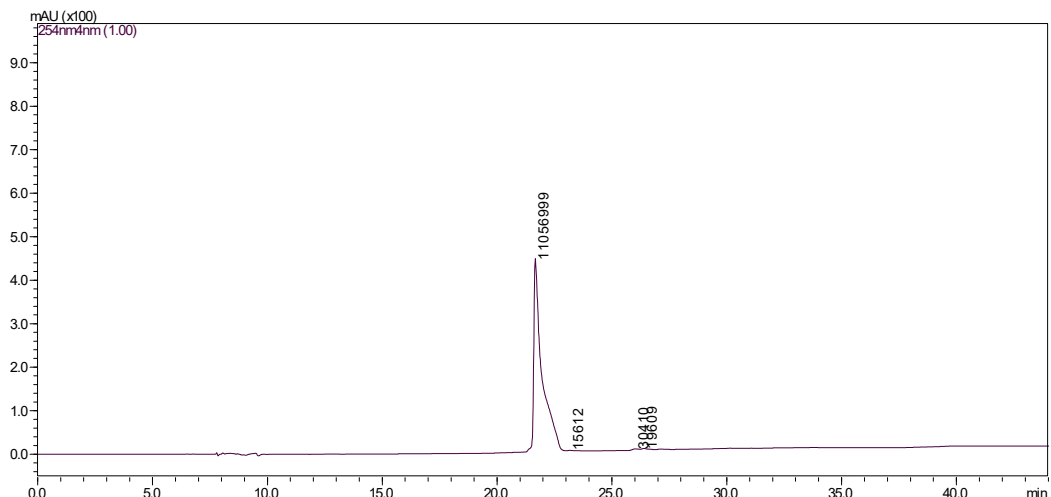


Figure S49. ESI-LCMS of compound geo105 after column chromatography purification

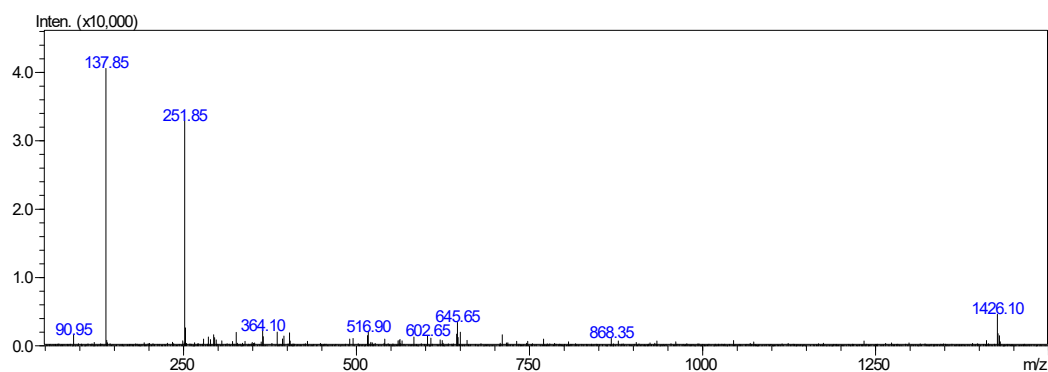


Figure S50. ESI-MS for geo105, negative mode: m/z calcd mass for $C_{70}H_{93}N_{17}O_{16} [M-H]^- = 1426.70$, was found 1426.10.

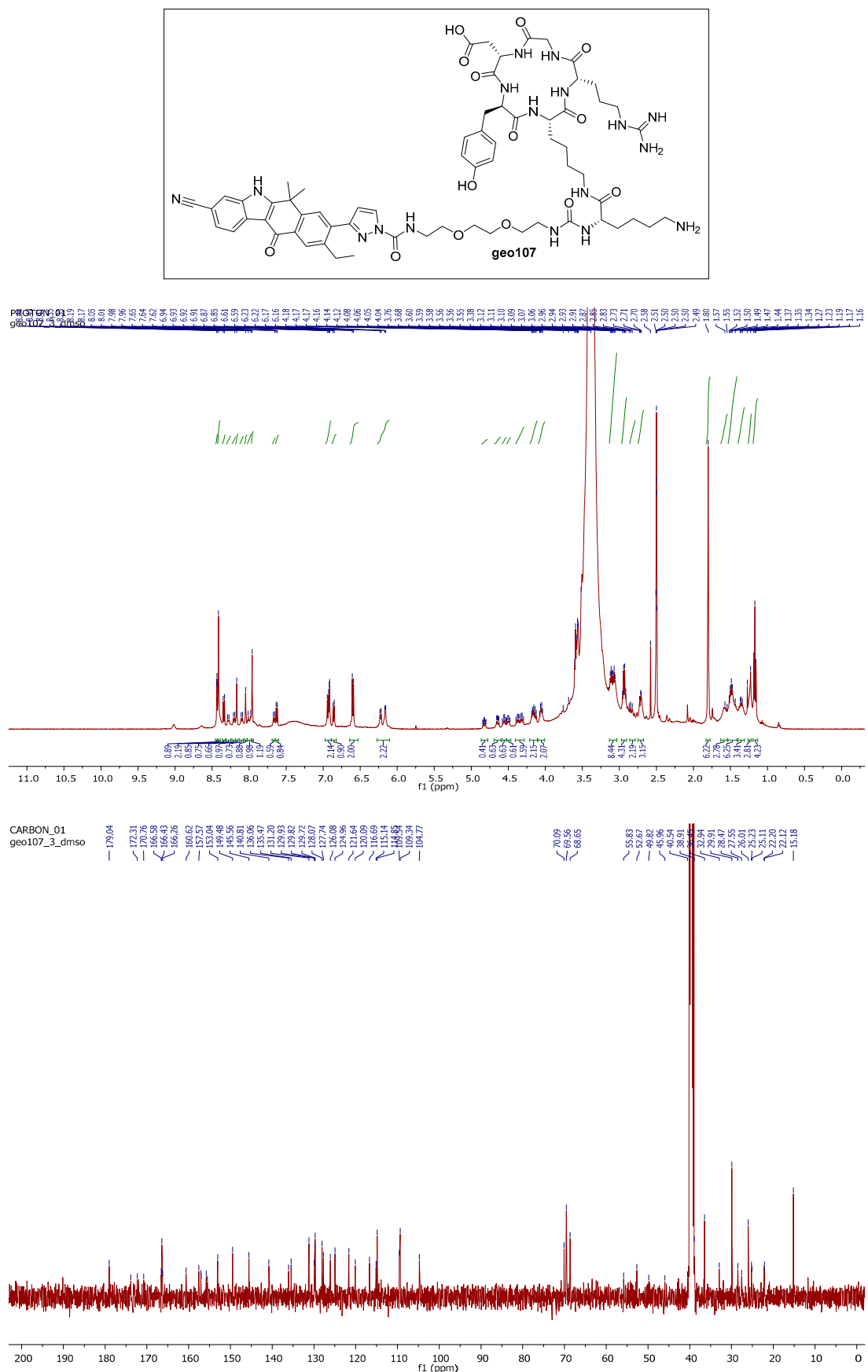
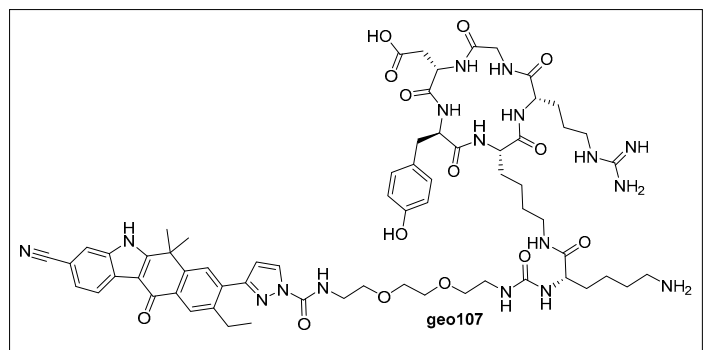


Figure S51. ^1H -NMR and ^{13}C -NMR spectra for compound **geo107**.



Method 1

Retention time: 18.8 m

area: 1819194 (absorbance units x minutes)

total area: 1855459 (absorbance units x minutes)

area %: $(1819194 / 1855459) * 100 = 98.0 \%$

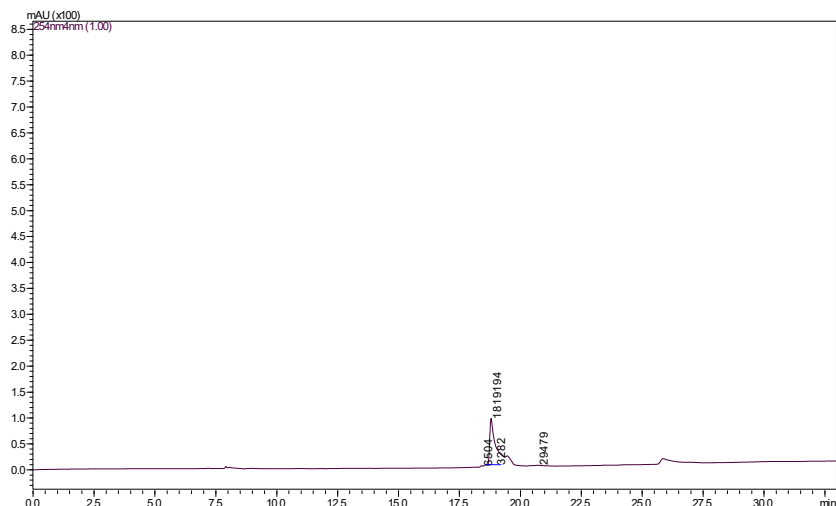


Figure S52. ESI-LCMS of compound geo107 after HPLC purification

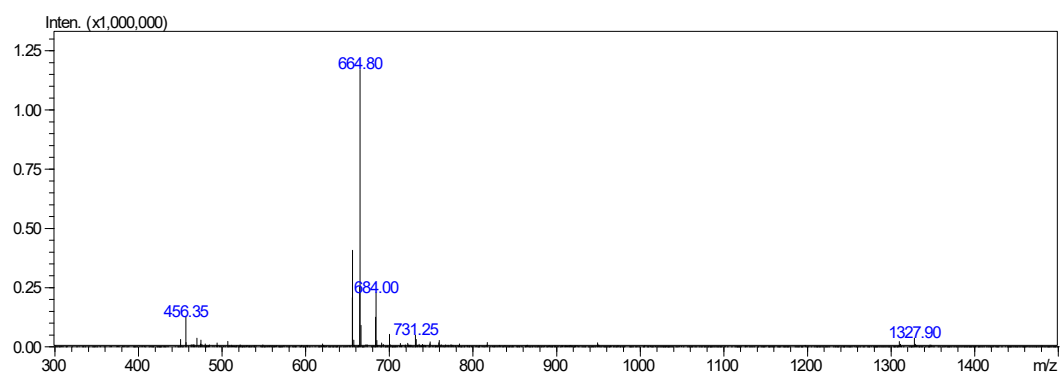


Figure S53. ESI-MS for geo107, positive mode: m/z calcd mass for $C_{65}H_{86}N_{17}O_{14}$ $[M+H]^+$ = 1328.65, was found 1327.9.

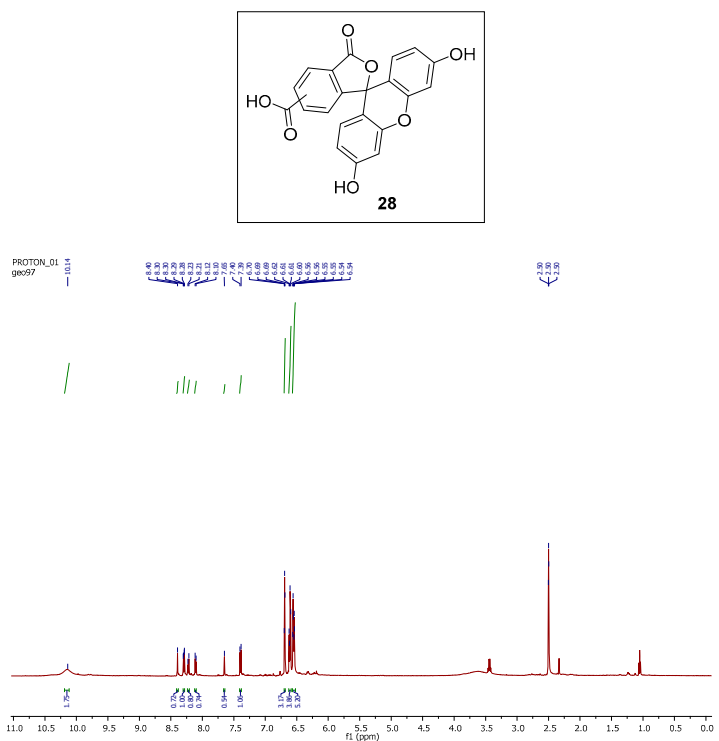


Figure S54. ¹H-NMR spectrum for compound 28.

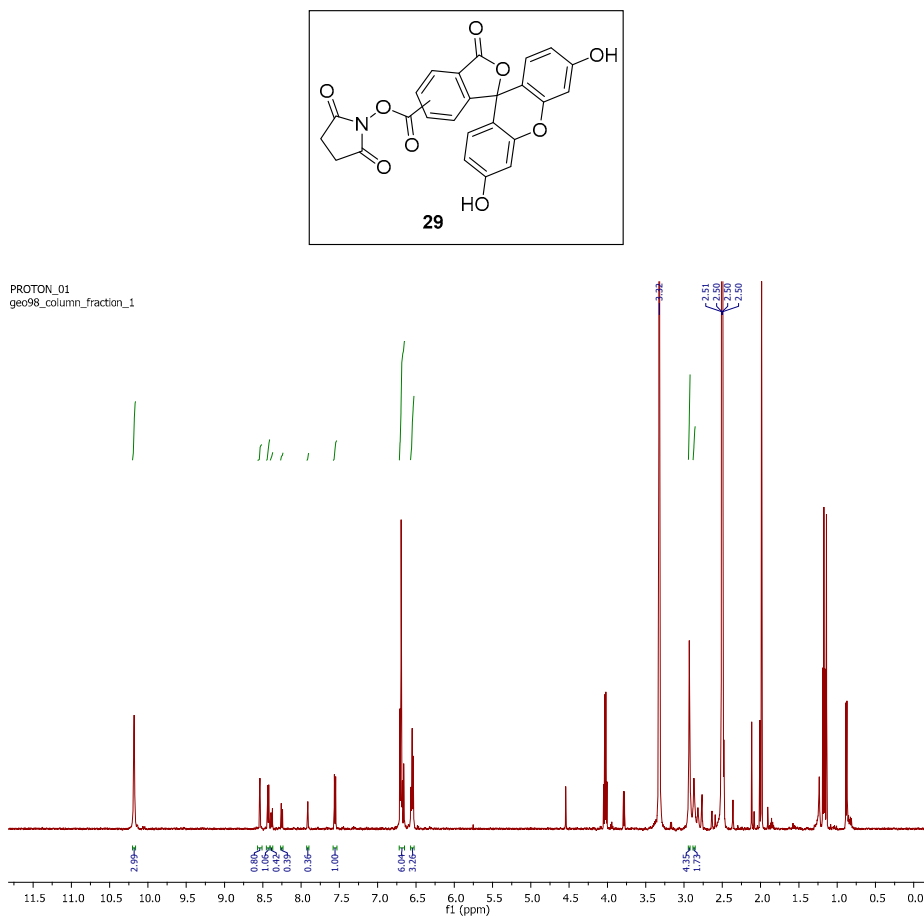
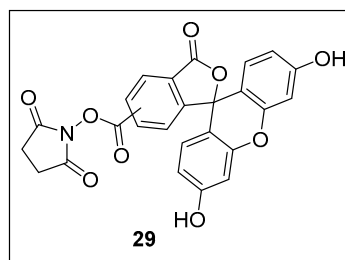


Figure S55. ¹H-NMR spectrum for compound 29.



Method 1

Retention time: 22.6 m

area: 19307526 (absorbance units x minutes)

total area: 20715865 (absorbance units x minutes)

area %: $(19307526/20715865)*100 = 93.2 \%$

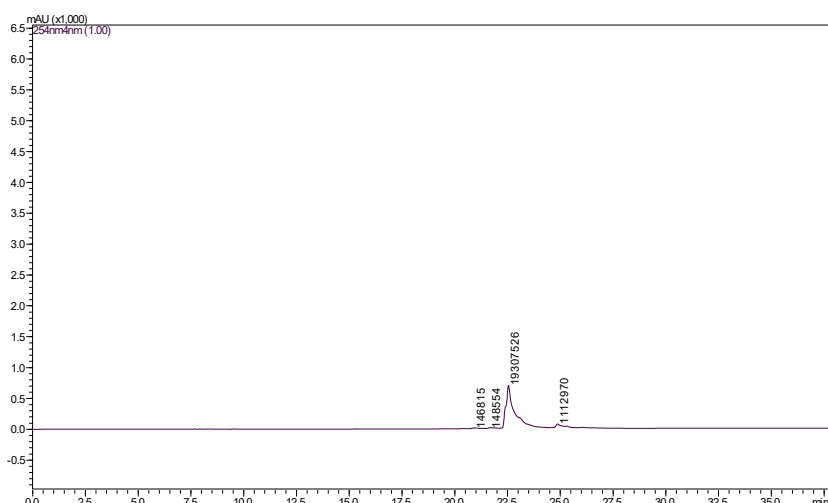


Figure S56. ESI-LCMS of compound **29** after column chromatography purification

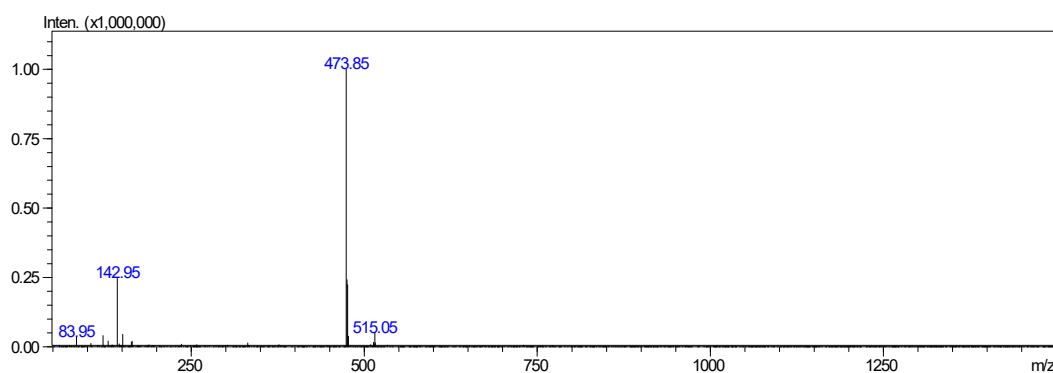


Figure S57. ESI-MS for **29**, positive mode: m/z calcd mass for $C_{25}H_{15}NO_9 [M]^+$ = 473.07, was found 473.85.

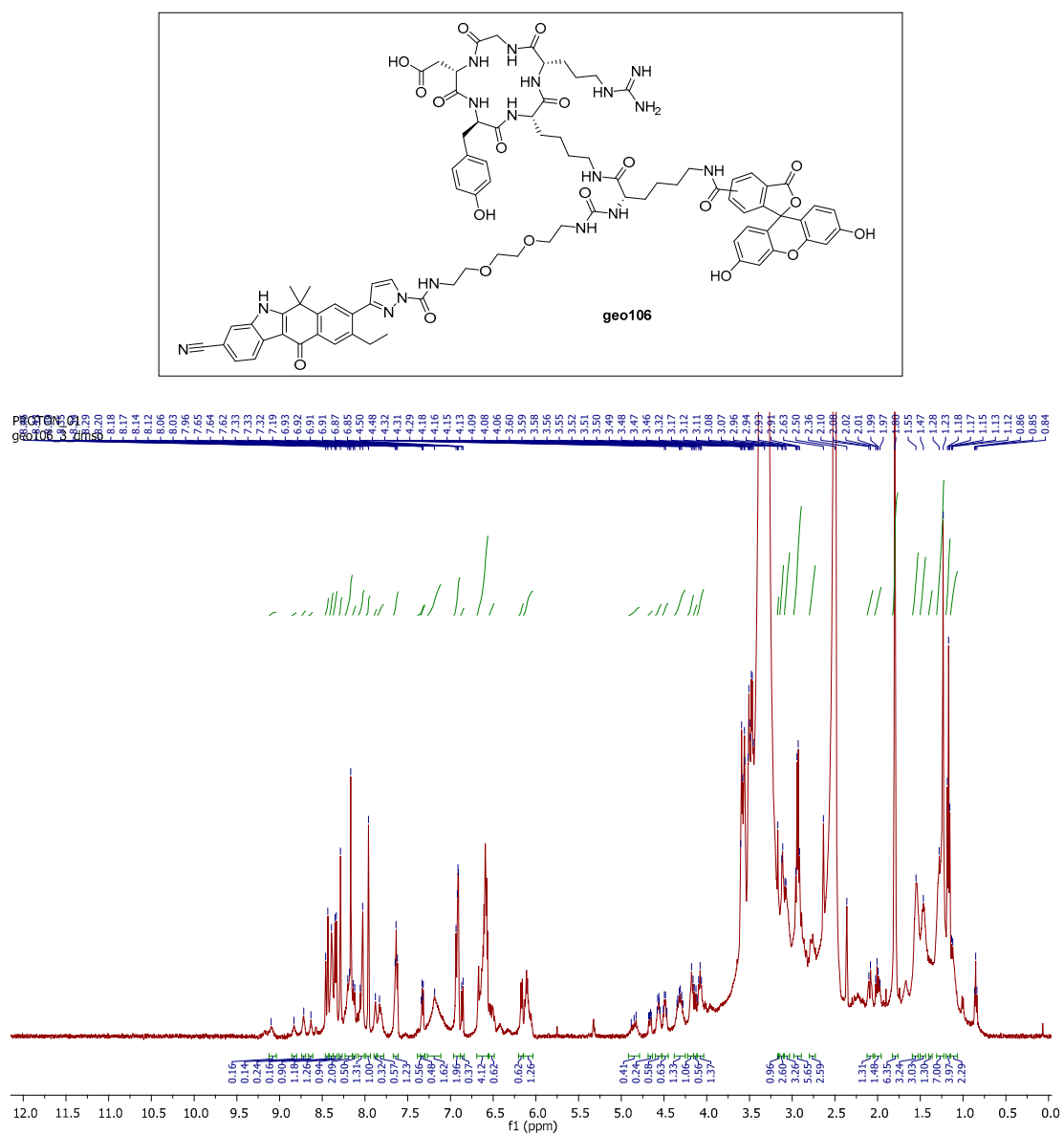
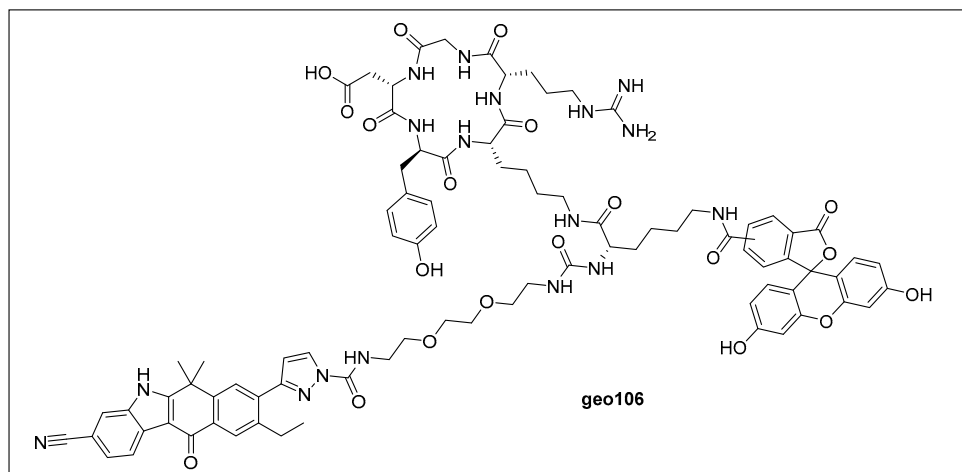


Figure S58. ^1H -NMR spectrum for compound geo106.



Method 5

Retention time: 21.3 m

area: 12951299 (absorbance units x minutes)

total area: 13466339 (absorbance units x minutes)

area %: $(12951299 / 13466339) * 100 = 96.1\%$

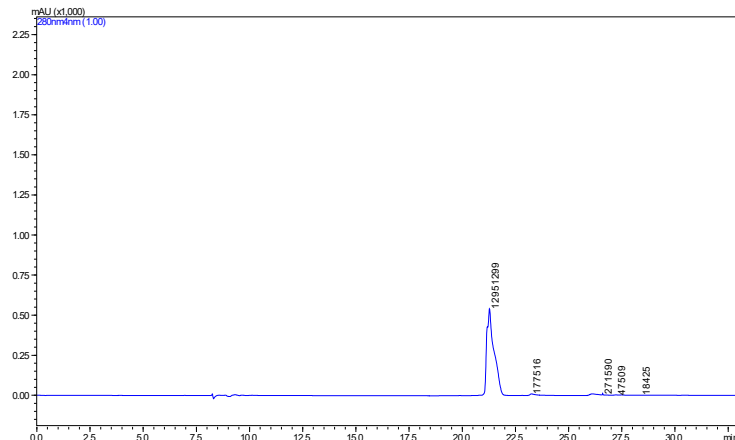


Figure S59. ESI-LCMS of compound **geo106** after HPLC purification

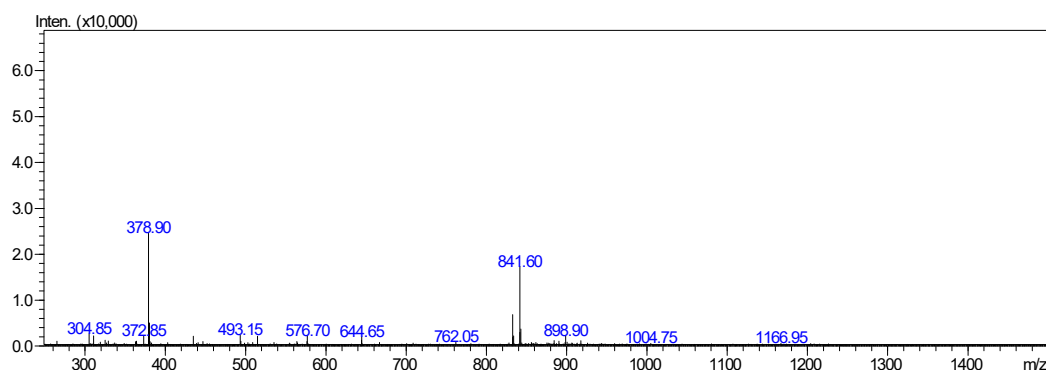


Figure S60. ESI-MS for **geo106**, negative mode: m/z calcd mass for $C_{86}H_{95}N_{17}O_{20}$ [$M/2-H^-$] = 841.84, was found 841.60.

Chemostability Studies

Compound geo75

➤ pH = 5.2, method 4

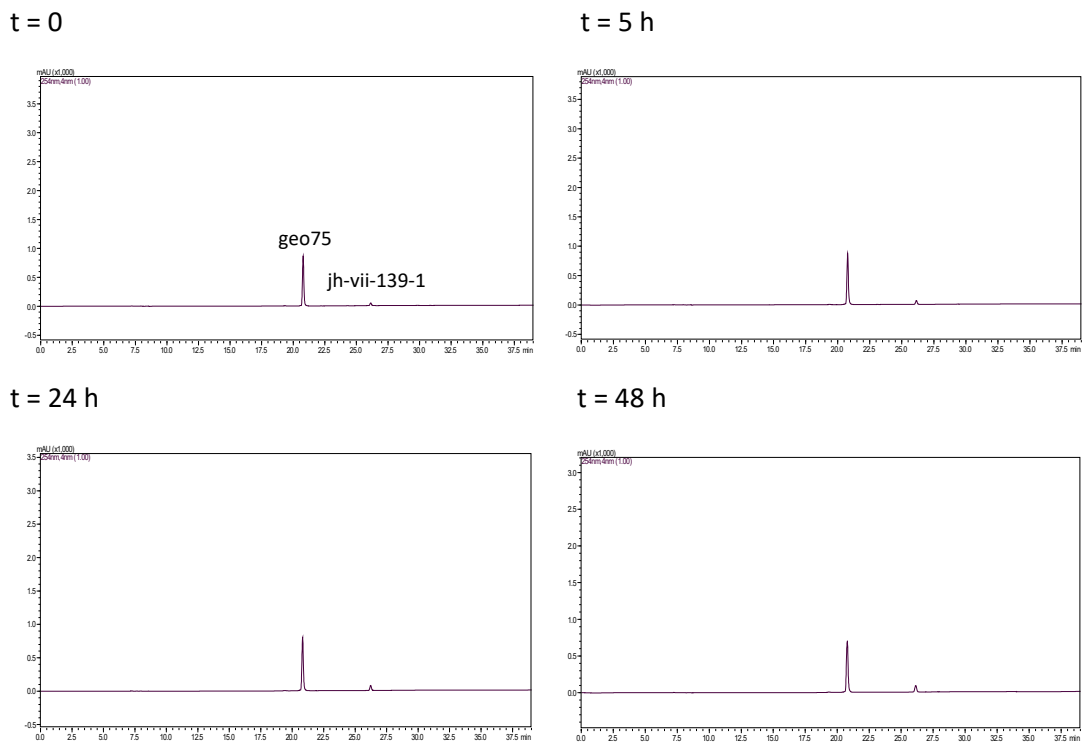


Figure S61. Stability of compound geo75 at pH=5.2.

➤ pH = 7.4, method 4

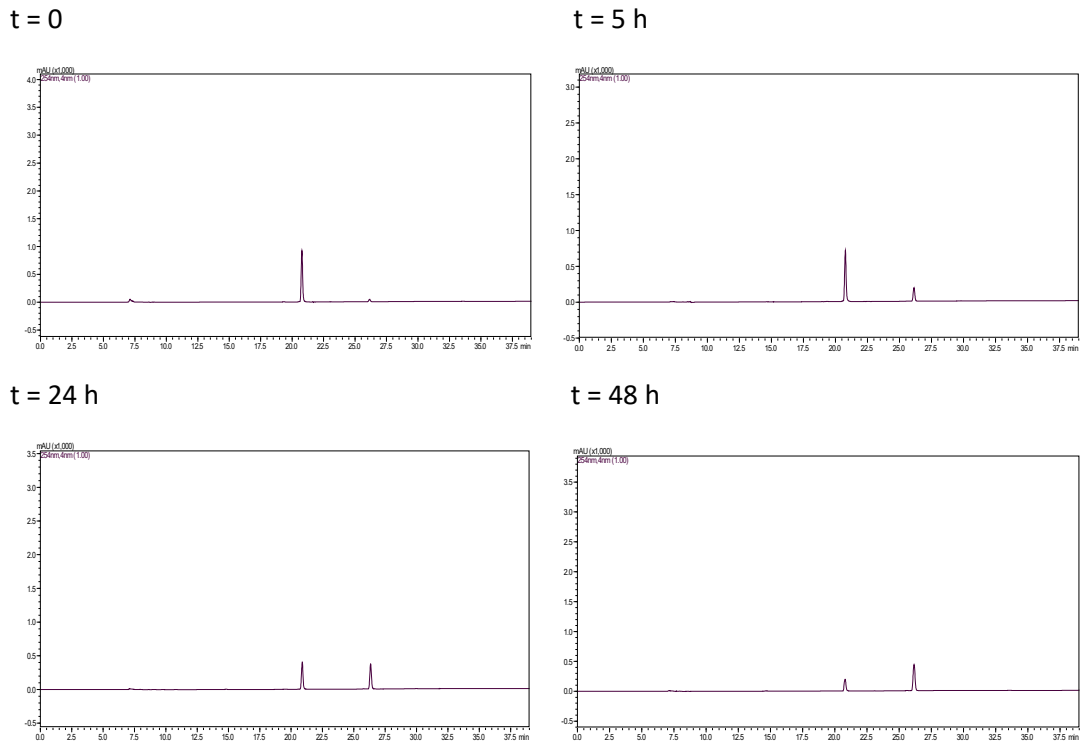


Figure S62. Stability of compound geo75 at pH=7.4.

➤ DMEM, method 4

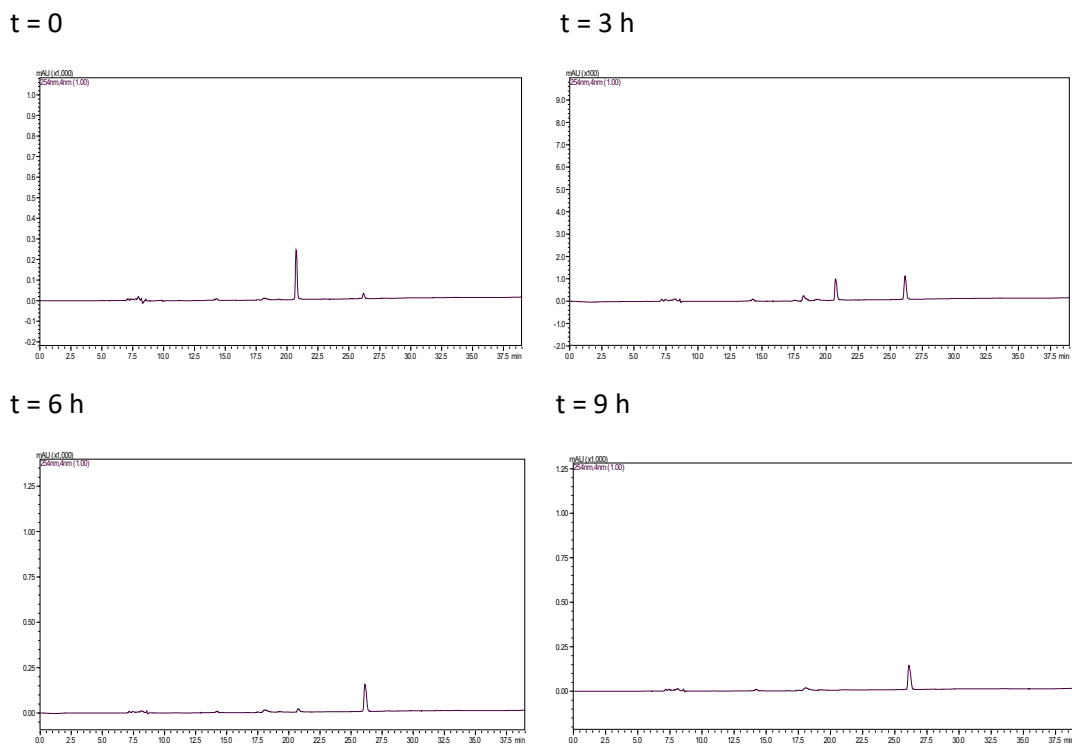


Figure S63. Stability of compound geo75 in DMEM.

➤ Human Plasma, method 2

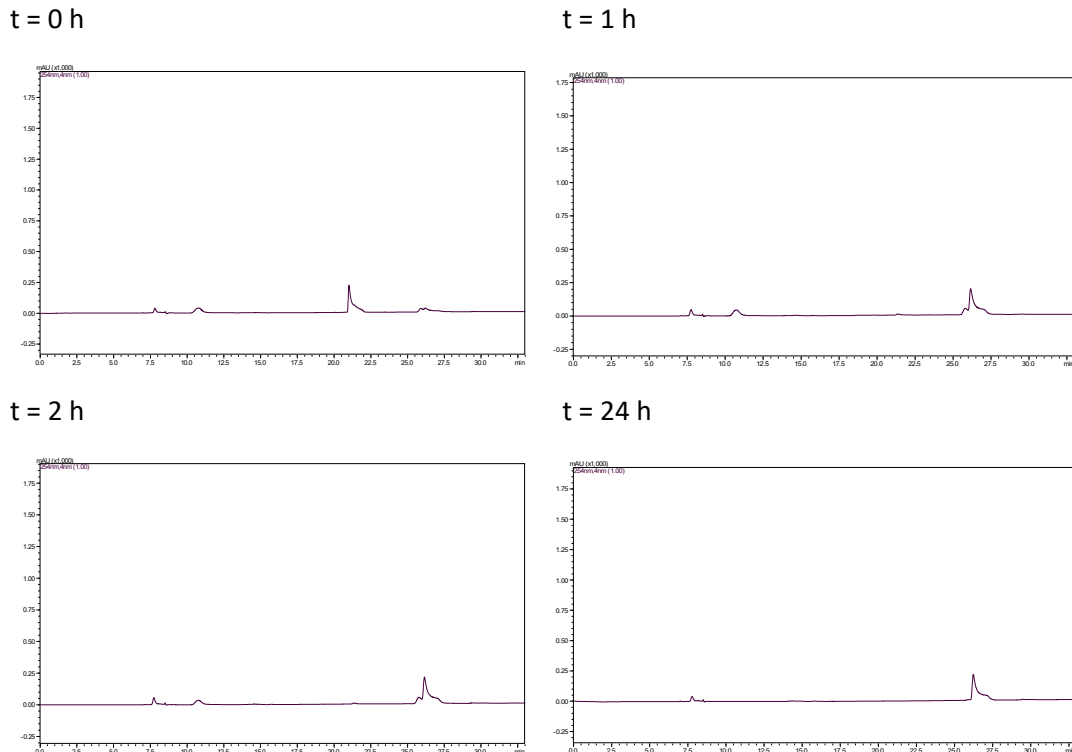
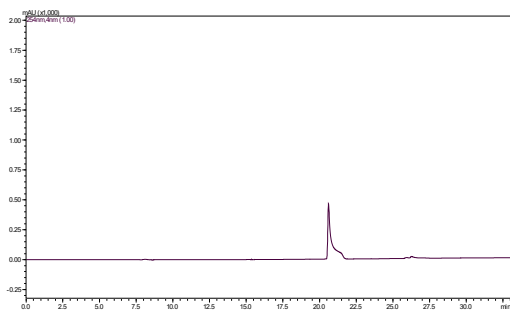


Figure S64. Stability of compound geo75 in human plasma.

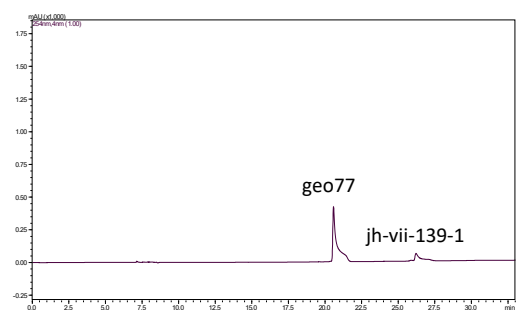
Compound geo77

➤ pH = 5.2, method 2

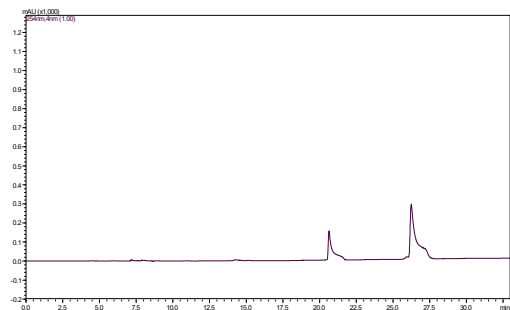
t = 0 h



t = 5 h



t = 24 h



t = 48 h

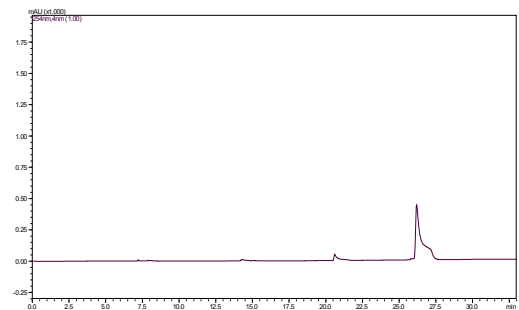
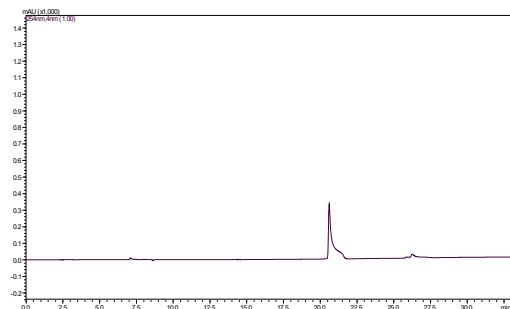


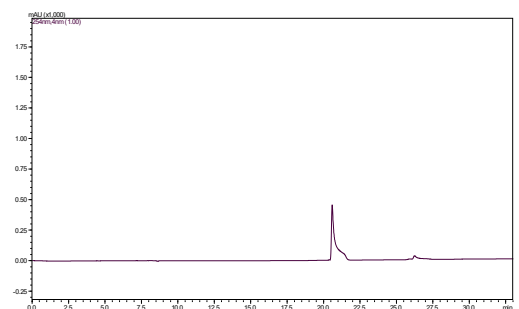
Figure S65. Stability of compound geo77 at pH=5.2.

➤ pH = 7.4, method 2

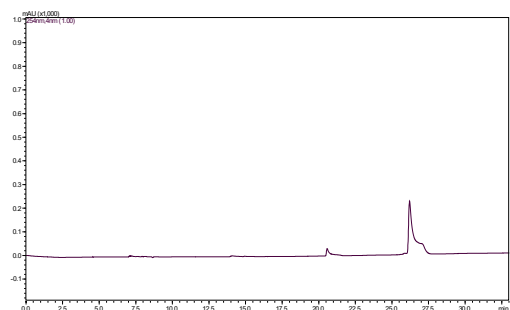
t = 0 h



t = 2 h



t = 5 h



t = 24 h

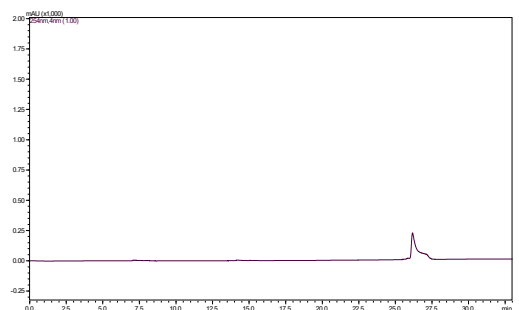
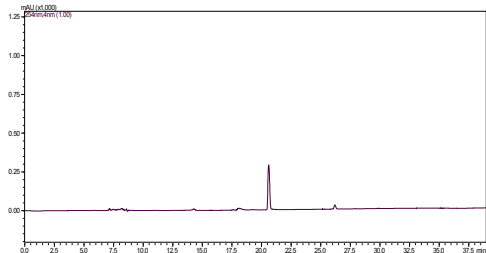


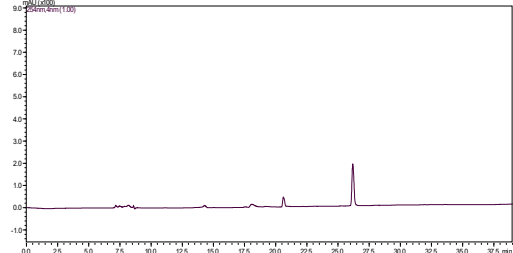
Figure S66. Stability of compound geo77 at pH=7.4.

➤ DMEM, method 4

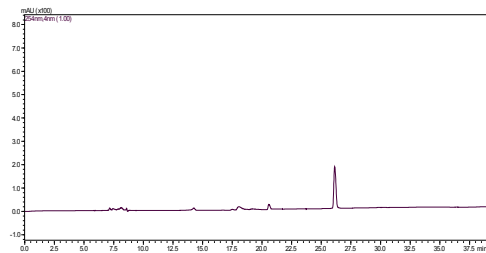
$t = 0\text{ h}$



$t = 1.5\text{ h}$



$t = 3\text{ h}$



$t = 7.5\text{ h}$

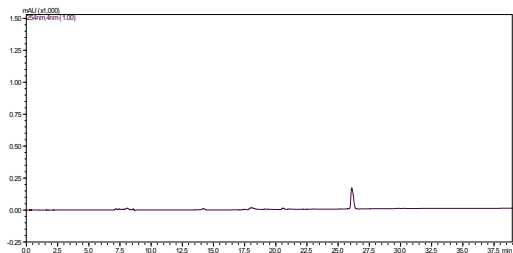
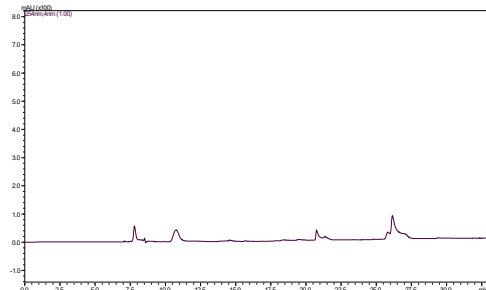


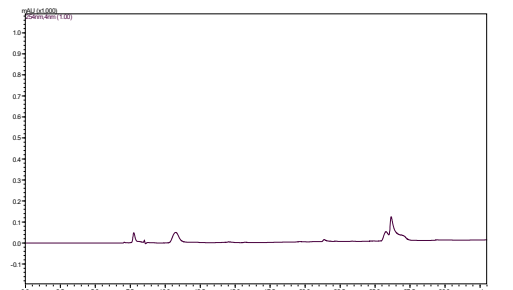
Figure S67. Stability of compound geo77 in DMEM.

➤ Human Plasma, method 2

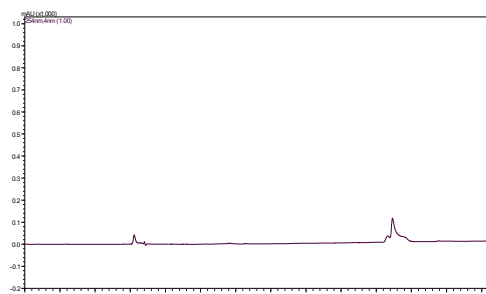
$t = 0\text{ h}$



$t = 1\text{ h}$



$t = 2\text{ h}$



$t = 24\text{ h}$

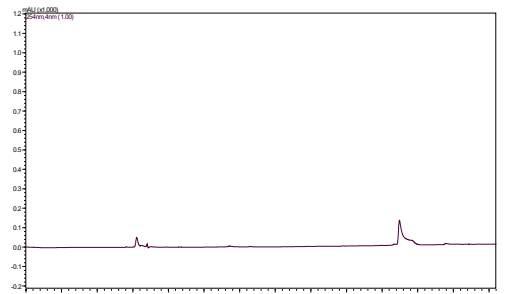
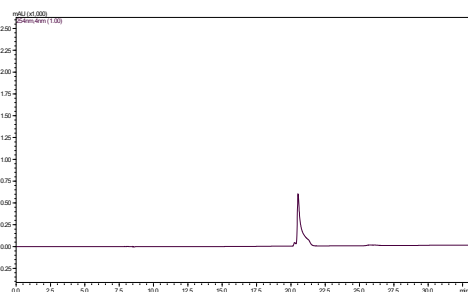


Figure S68. Stability of compound geo77 in human plasma.

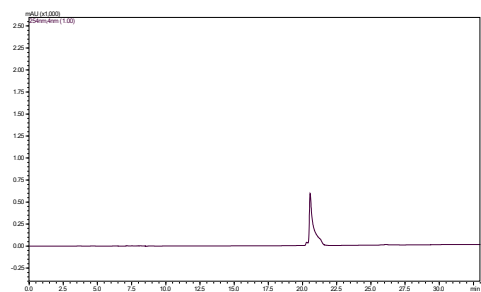
Compound geo85

➤ pH = 5.2, method 2

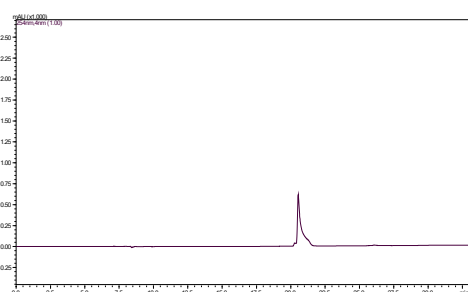
t = 0 h



t = 3 h



t = 5 h



t = 48 h

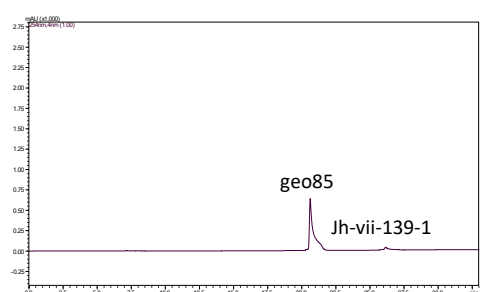
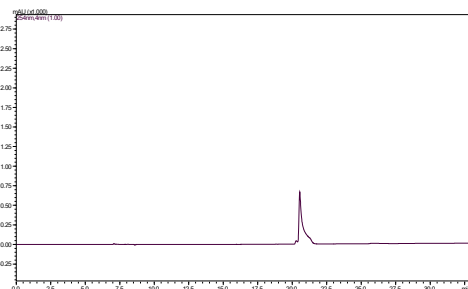


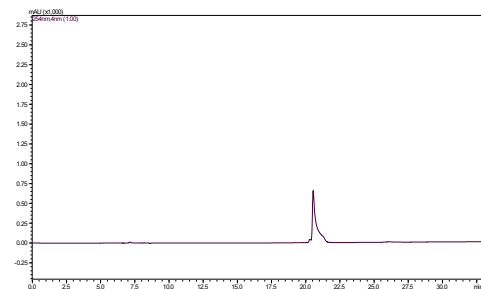
Figure S69. Stability of compound geo85 at pH=5.2.

➤ pH = 7.4, method 2

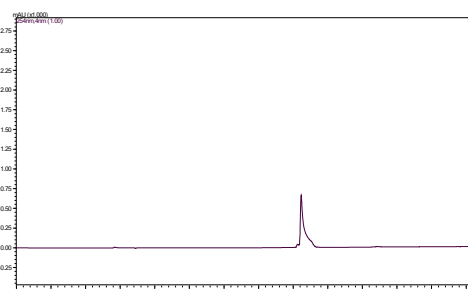
t = 0 h



t = 3 h



t = 5 h



t = 48 h

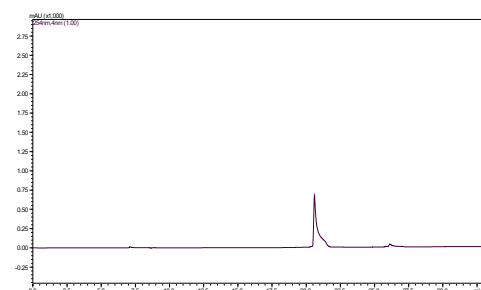


Figure S70. Stability of compound geo85 at pH=7.4.

➤ DMEM, method.2

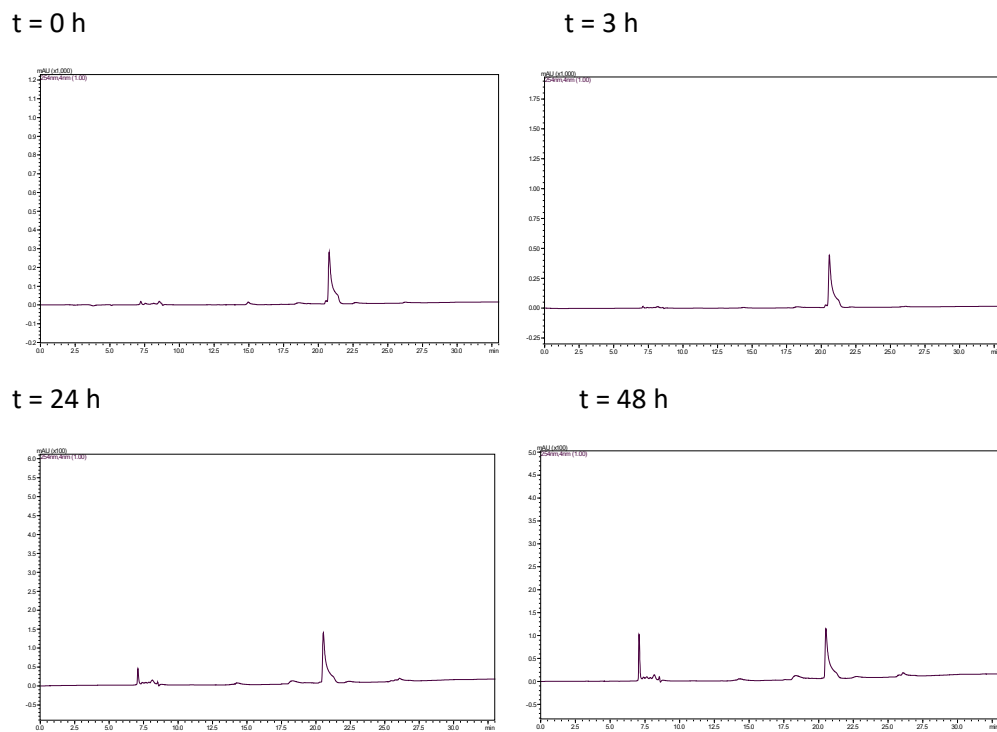


Figure S71. Stability of compound geo85 in DMEM.

➤ Human Plasma, method 1

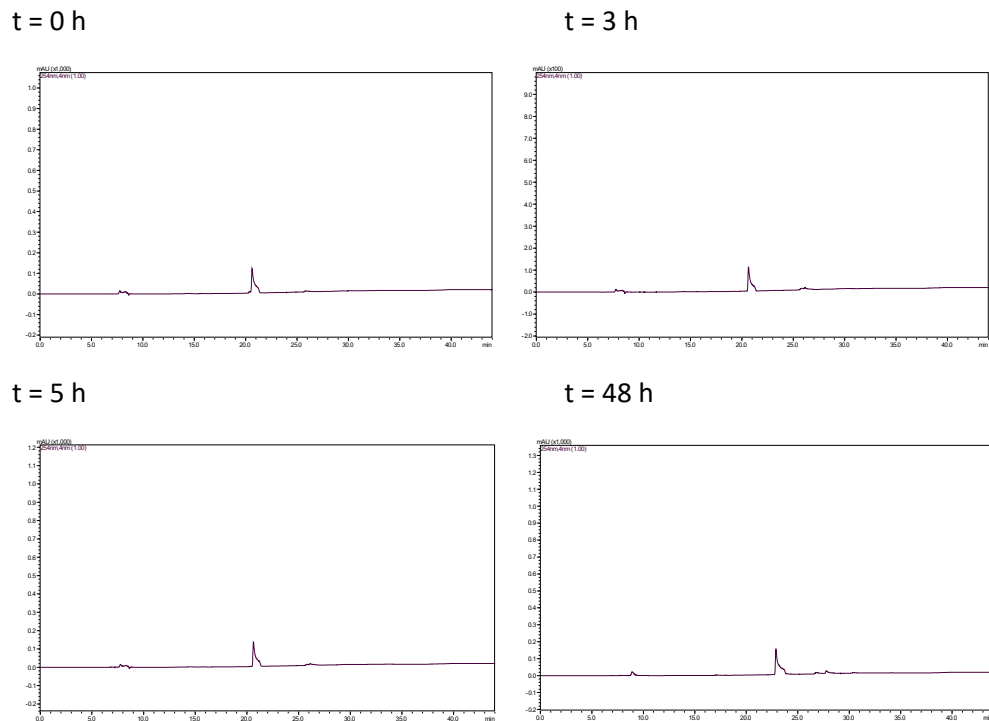
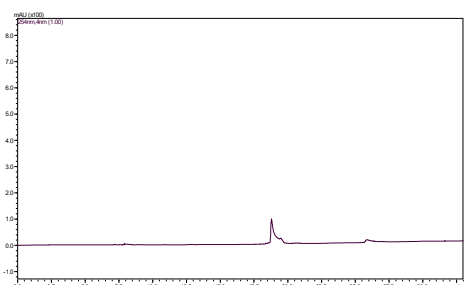


Figure S72. Stability of compound geo85 in human plasma.

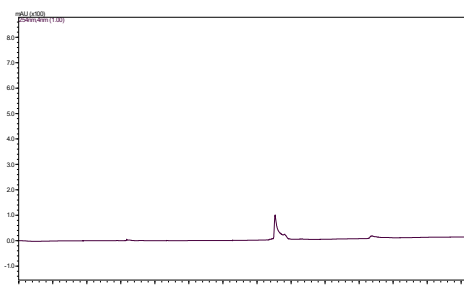
Compound geo107

➤ pH = 5.2, method 2

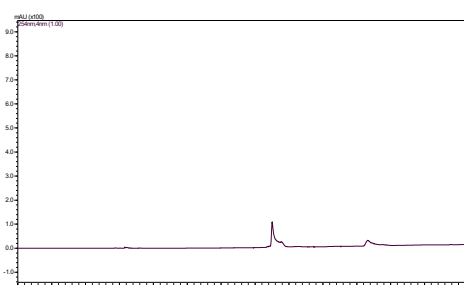
t = 0 h



t = 3 h



t = 5 h



t = 24 h

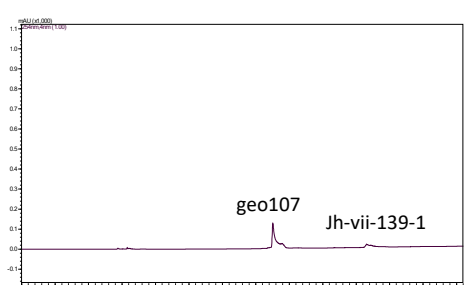
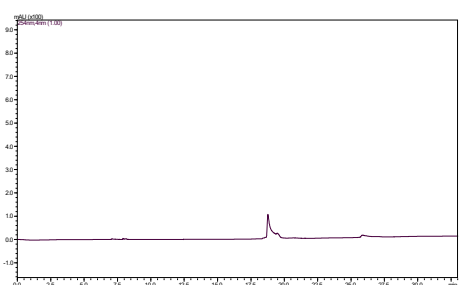


Figure S73. Stability of compound geo107 at pH=5.2.

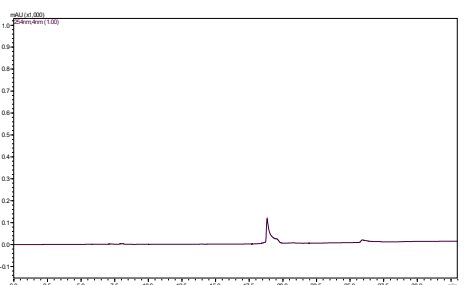
Compound geo107

➤ pH = 7.4, method 2

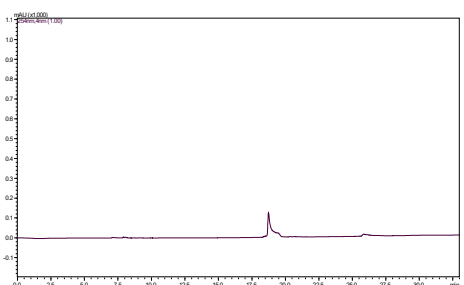
t = 0 h



t = 3 h



t = 5 h



t = 24 h

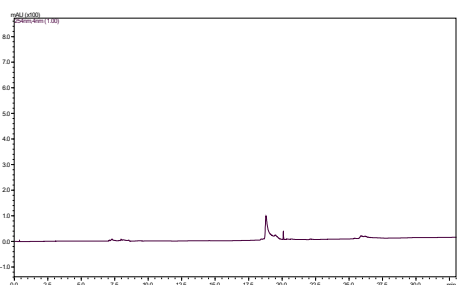
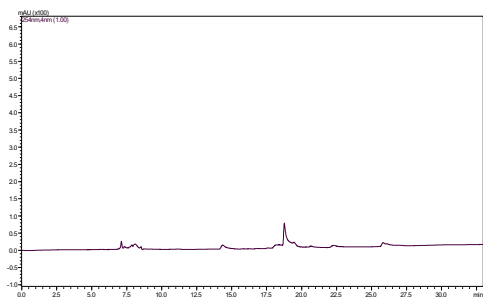


Figure S74. Stability of compound geo107 at pH=7.4.

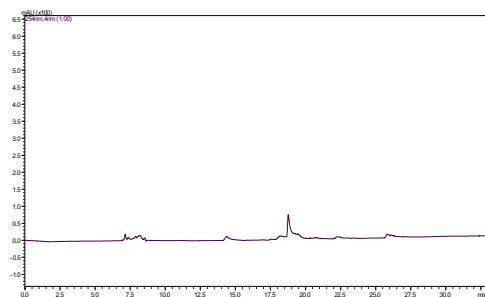
Compound geo107

➤ DMEM, method 2

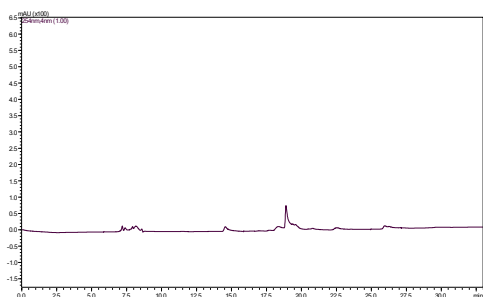
t = 0 h



t = 2 h



t = 5 h



t = 48 h

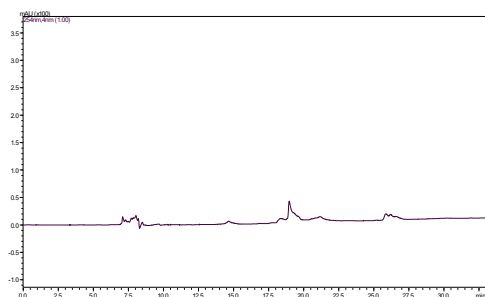
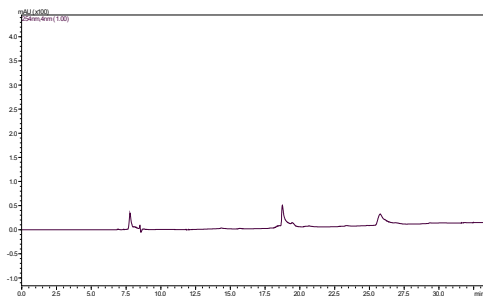


Figure S75. Stability of compound geo107 in DMEM.

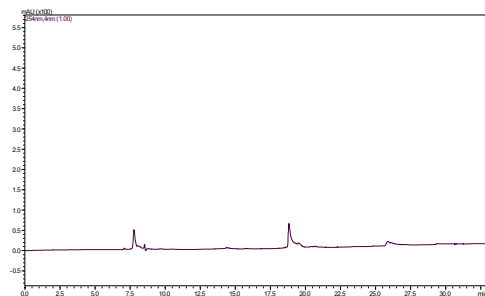
Compound geo107

➤ Human Plasma, method 2

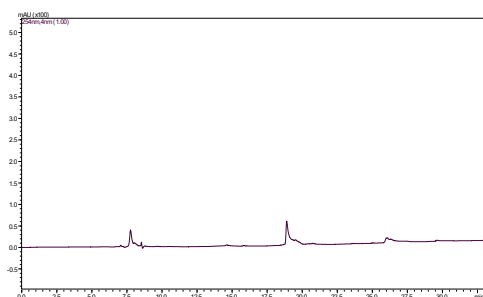
t = 0 h



t = 2 h



t = 5 h



t = 48 h

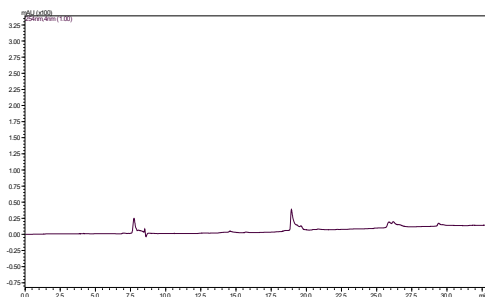
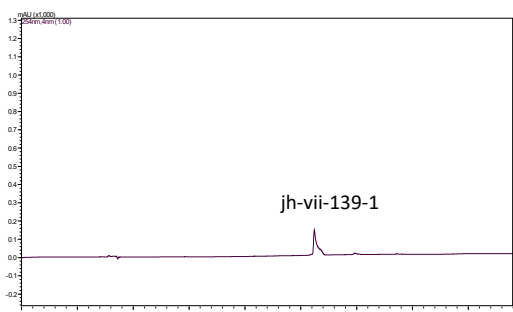


Figure S76. Stability of compound geo107 in human plasma.

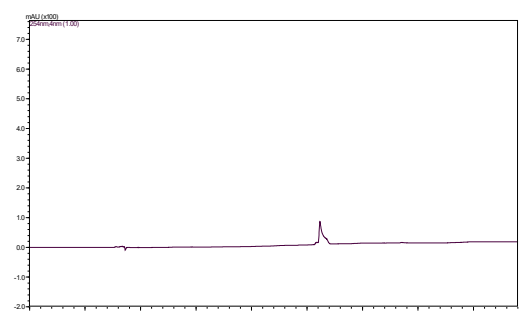
Compound JH-VII-139-1

➤ DMEM, method 1

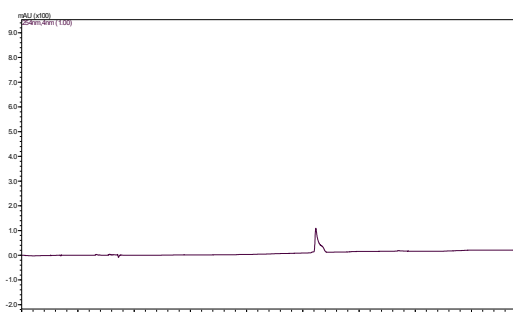
t = 0 h



t = 2 h



t = 24 h



t = 48 h

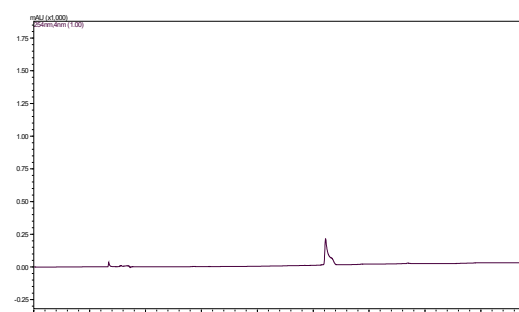
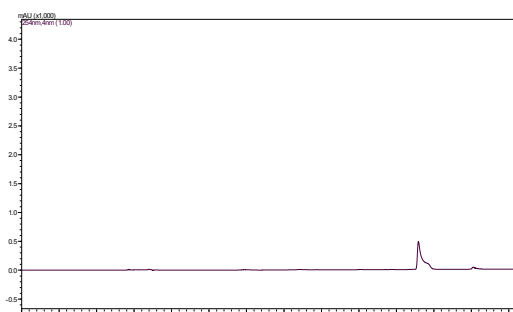


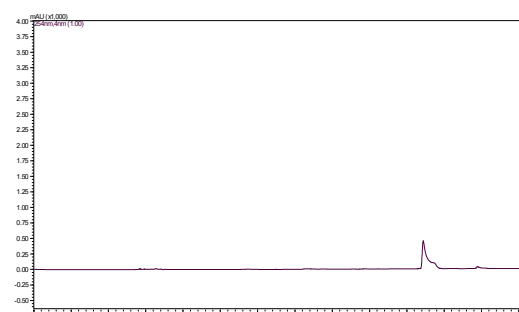
Figure S77. Stability of compound JH-VII-139-1 in DMEM.

➤ Human Plasma, method 2

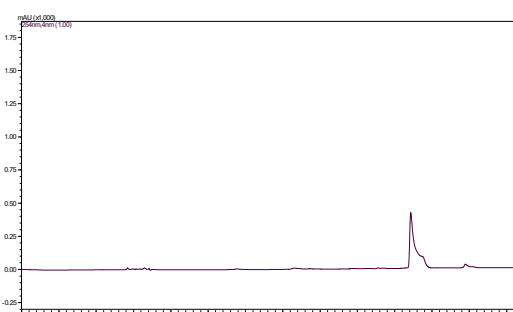
t = 0 h



t = 3 h



t = 5 h



t = 48 h

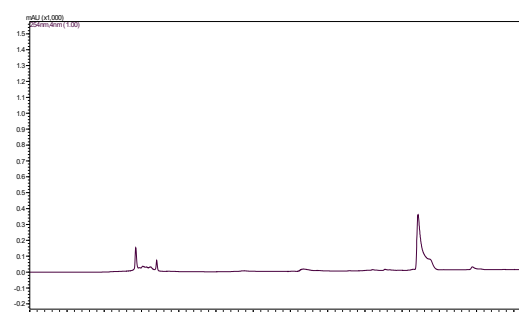


Figure S78. Stability of compound JH-VII-139-1 in human plasma.

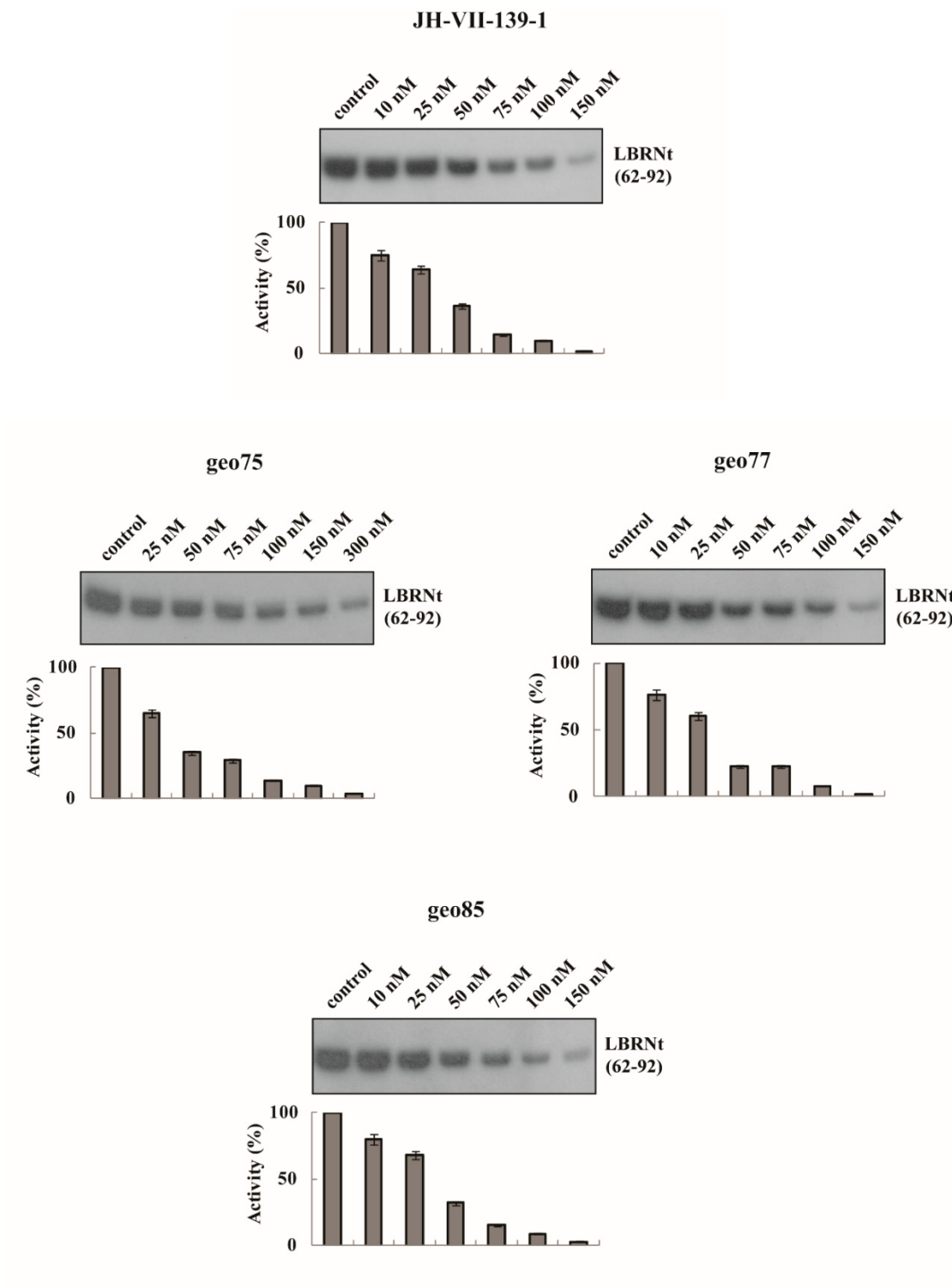


Figure S79. In vitro phosphorylation of GST-LBRNt(62-92) by GST-SRPK1 in the presence of increasing concentrations (10-300 nM) of JH-VII-139-1, geo75, geo77 and geo85 respectively. Phosphorylated bands were excised from the dry gel and Cherenkov counted.